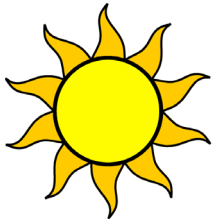

Predictive Science, Inc.

THERMAL NONEQUILIBRIUM IN CORONAL LOOPS

Zoran Mikić

Cooper Downs

Roberto Lionello

Jon A. Linker

Predictive Science, Inc., San Diego, CA, USA

Amy Winebarger

NASA Marshall Space Flight Center, Huntsville, AL, USA

Presented at the 8th Coronal Loops Workshop, Palermo, Italy, June 27–30, 2017

Supported by NASA's HSR Program

INTRODUCTION

- Thermal nonequilibrium may play an important role in the dynamics of coronal loops
- The wide variation in observed coronal loop properties implies that several physical mechanisms are likely to be active
- Inferences from spectroscopic observations of high coronal temperatures ($\gtrsim$ 3–4 MK) in active-region loops imply that intense bursts of heating are occurring (e.g., nanoflares)
- Energy deposition events, such as nanoflares, on a time scale faster than the loop cooling time would appear as quasistatic heating
- It is probable that coronal emission may involve a combination of thermal nonequilibrium and nanoflare heating, as well as other effects (slow evolution of **B**, significant reconfiguration of **B**, etc.), on multiple length and time scales
- We study thermal nonequilibrium not because it is necessarily the principal effect, but because it may play a significant role in coronal emission

INTRODUCTION

- Thermal nonequilibrium may play an important role in the dynamics of coronal loops
- The wide variation in observed coronal loop properties implies that several physical mechanisms are likely to be active
- Inferences from spectroscopic observations of high coronal temperatures ($\gtrsim$ 3–4 MK) in active-region loops imply that intense bursts of heating are occurring (e.g., nanoflares)
- Energy deposition events, such as nanoflares, on a time scale faster than the loop cooling time would appear as quasistatic heating
- It is probable that coronal emission may involve a combination of thermal nonequilibrium and nanoflare heating, as well as other effects (slow evolution of **B**, significant reconfiguration of **B**, etc.), on multiple length and time scales
- We study thermal nonequilibrium not because it is necessarily the principal effect, but because it may play a significant role in coronal emission

THERMAL NONEQUILIBRIUM

- Generally defined as an absence of steady-state solutions of the hydrodynamic equations that govern coronal loop dynamics, even for steady heating
- This can happen generally, but also in 1D models, where it is easiest to study
- The nonlinear interplay of heat conduction, radiative loss, and coronal heating produces very rich and complex behavior
- In such cases, the solutions to the time-dependent equations exhibit oscillatory behavior that often cycle in time
- The solutions typically have cycles on ~ hour time scales (for typical loop lengths and parameters)
- Heating profiles that are concentrated near the loop footpoints (so-called “footpoint heating”) tend to produce thermal nonequilibrium
- This possibility was already recognized early on in the Skylab era (e.g., Rosner, Tucker, & Vaiana 1978)

1D Loop Equations

$$\frac{\partial \rho}{\partial t} + v\frac{\partial \rho}{\partial s} = -\rho \frac{1}{A}\frac{\partial}{\partial s}(Av)$$

$$\frac{\partial v}{\partial t} + v\frac{\partial v}{\partial s} = -\frac{1}{\rho}\frac{\partial p}{\partial s} + g_s$$

$$\frac{\partial T}{\partial t} + v\frac{\partial T}{\partial s} = -(\gamma - 1)T\frac{1}{A}\frac{\partial}{\partial s}(Av) + \frac{(\gamma - 1)}{2kn_e}\left[\frac{1}{A}\frac{\partial}{\partial s}\left(A\kappa_{\parallel}\frac{\partial T}{\partial s}\right) - n_e^2 Q(T) + H\right]$$

1D Loop Equations

$$\frac{\partial \rho}{\partial t} + v\frac{\partial \rho}{\partial s} = -\rho \frac{1}{A}\frac{\partial}{\partial s}(Av)$$

$$\frac{\partial v}{\partial t} + v\frac{\partial v}{\partial s} = -\frac{1}{\rho}\frac{\partial p}{\partial s} + g_s$$

$$\frac{\partial T}{\partial t} + v\frac{\partial T}{\partial s} = -(\gamma - 1)T\frac{1}{A}\frac{\partial}{\partial s}(Av) + \frac{(\gamma - 1)}{2kn_e}\left[\frac{1}{A}\frac{\partial}{\partial s}\left(A\kappa_{\parallel}\frac{\partial T}{\partial s}\right) - n_e^2 Q(T) + H\right]$$

OBSERVATIONAL CONSEQUENCES OF THERMAL NONEQUILIBRIUM

- Thermal nonequilibrium tends to produce long time lags between intensity peaks in different EUV channels (Winebarger *et al*. 2016, 2017), providing possibilities to better fit observations (Ugarte-Urra *et al*. 2006) [see Amy Winebarger's talk later today]
- Thermal nonequilibrium may play a key role in the formation and evolution of filaments/prominences (Luna *et al*. 2012; Xia *et al*. 2014) [see Roberto Lionello's poster later today]
- It has been argued that observed loop pulsations with periods of several hours may be manifestations of thermal nonequilibrium (Auchère *et al*. 2014; Froment *et al*. 2015, 2017) [see Clara Froment's and Frédéric Auchère's talks later today]
- Full condensations resulting from thermal nonequilibrium that fall down along the legs of coronal loops have been interpreted as coronal rain (e.g., DeGroof *et al*. 2004, 2005; Müller *et al*. 2005; Antolin *et al*. 2010, 2016; Antolin & Rouppe van der Voort 2012)

OBSERVATIONAL CONSEQUENCES OF THERMAL NONEQUILIBRIUM (CONT.)

- Klimchuk *et al*. (2010) have argued that thermal nonequilibrium does not agree with observations, but this may be because they only considered full condensations
- When more general types of solutions are considered, which we argue are more likely to occur in the corona, we see that thermal nonequilibrium solutions reproduce some characteristics of observed loops (e.g., Lionello *et al*. 2013; Winebarger *et al*. 2014)
- In fact, to explain certain observations it may be *necessary* to invoke thermal nonequilibrium (e.g., long time delays between emission channels, loop pulsations, enhanced EUV emission, etc.)
- The prevalence of thermal nonequilibrium in the corona, and particularly, incomplete vs. complete condensations, is a key point, but this may depend on the details of coronal heating [Jim Klimchuk has a poster related to this topic later today]

DIFFICULTIES IN INTERPRETING OBSERVATIONS

- Observations integrate the various contributions of multiple loops along the line of sight, and this can confound their interpretation [see the poster by Cooper Downs later today]
- The assumptions about loop area and geometry can have a significant effect on the dynamics and properties of loops (Mikić *et al*. 2013)
- Loop areas are defined by a magnetic model of the active region, but these are notoriously difficult to come by (e.g., NLFFF)

BEHAVIOR OF LOOPS FROM 3D AR MODELS

- Thermal nonequilibrium is prevalent in our 3D simulations of an active region, producing thin loops with rather uniform cross-sections in simulated EUV emission (Mok *et al*. 2016)
- This happens when the loops are heated to match emission in X-ray channels
- The heating was specified according to the scaling laws of Rappazzo & Velli (2008): $H = H_o B^{7/4} \rho^{1/8} L^{-3/4}$, and tends to be concentrated at the loop footpoints
- The stability of these loops is closely related to the cross-sectional area; loops with large values of A_{max}/A_{min} tend to be thermally unstable
- The properties of these loops compare well with the generic properties of observed loops (Lionello *et al*. 2013; Winebarger *et al*. 2014)

The Astrophysical Journal, 817:15 (16pp), 2016 January 20 doi:10.3847/0004-637X/817/1/15

A THREE-DIMENSIONAL MODEL OF ACTIVE REGION 7986: COMPARISON OF SIMULATIONS WITH OBSERVATIONS

Yung Mok[1], Zoran Mikić[2], Roberto Lionello[2], Cooper Downs[2], and Jon A. Linker[2]
[1] Department of Physics and Astronomy, University of California, Irvine, CA 92697, USA; ymok@uci.edu
[2] Predictive Science, Inc., San Diego, CA 92121, USA
Received 2015 April 10; accepted 2015 November 24; published 2016 January 19

ABSTRACT

In the present study, we use a forward modeling method to construct a 3D thermal structure encompassing active region 7986 of 1996 August. The extreme ultraviolet (EUV) emissions are then computed and compared with observations. The heating mechanism is inspired by a theory on Alfvén wave turbulence dissipation. The magnetic structure is built from a *Solar and Heliospheric Observatory* (*SOHO*)/MDI magnetogram and an estimated torsion parameter deduced from observations. We found that the solution to the equations in some locations is in a thermal nonequilibrium state. The time variation of the density and temperature profiles leads to time dependent emissions, which appear as thin, loop-like structures with uniform cross-section. Their timescale is consistent with the lifetime of observed coronal loops. The dynamic nature of the solution also leads to plasma flows that resemble observed coronal rain. The computed EUV emissions from the coronal part of the fan loops and the high loops compare favorably with *SOHO*/EIT observations in a quantitative comparison. However, the computed emission from the lower atmosphere is excessive compared to observations, a symptom common to many models. Some factors for this discrepancy are suggested, including the use of coronal abundances to compute the emissions and the neglect of atmospheric opacity effects.

Key words: Sun: atmosphere – Sun: corona – Sun: UV radiation

Supporting material: animations

Simulated EIT171Å Emission from AR7986 (August 1996)

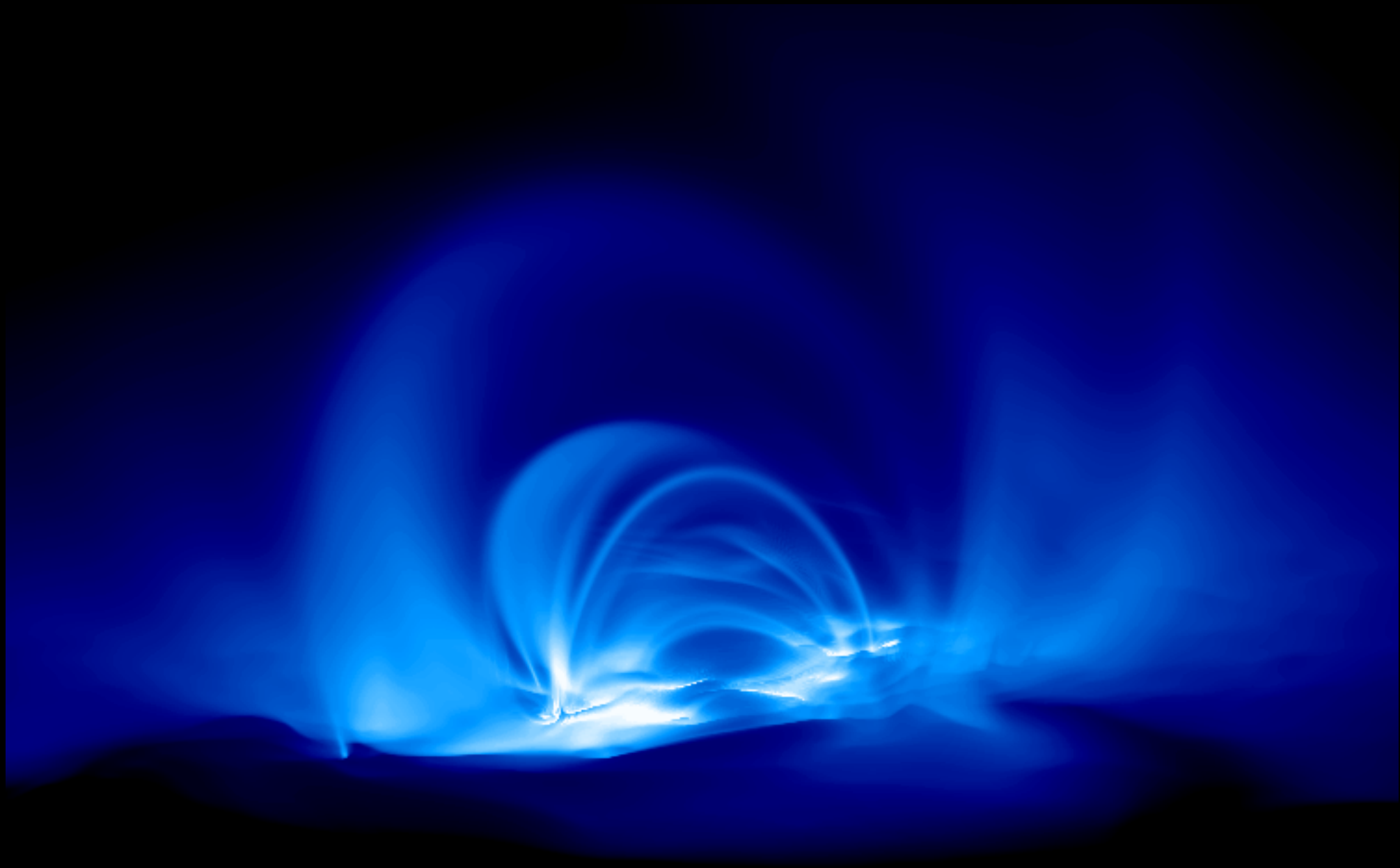

Case 979, seq # 100

Simulated EIT171Å Emission from AR7986 (August 1996)

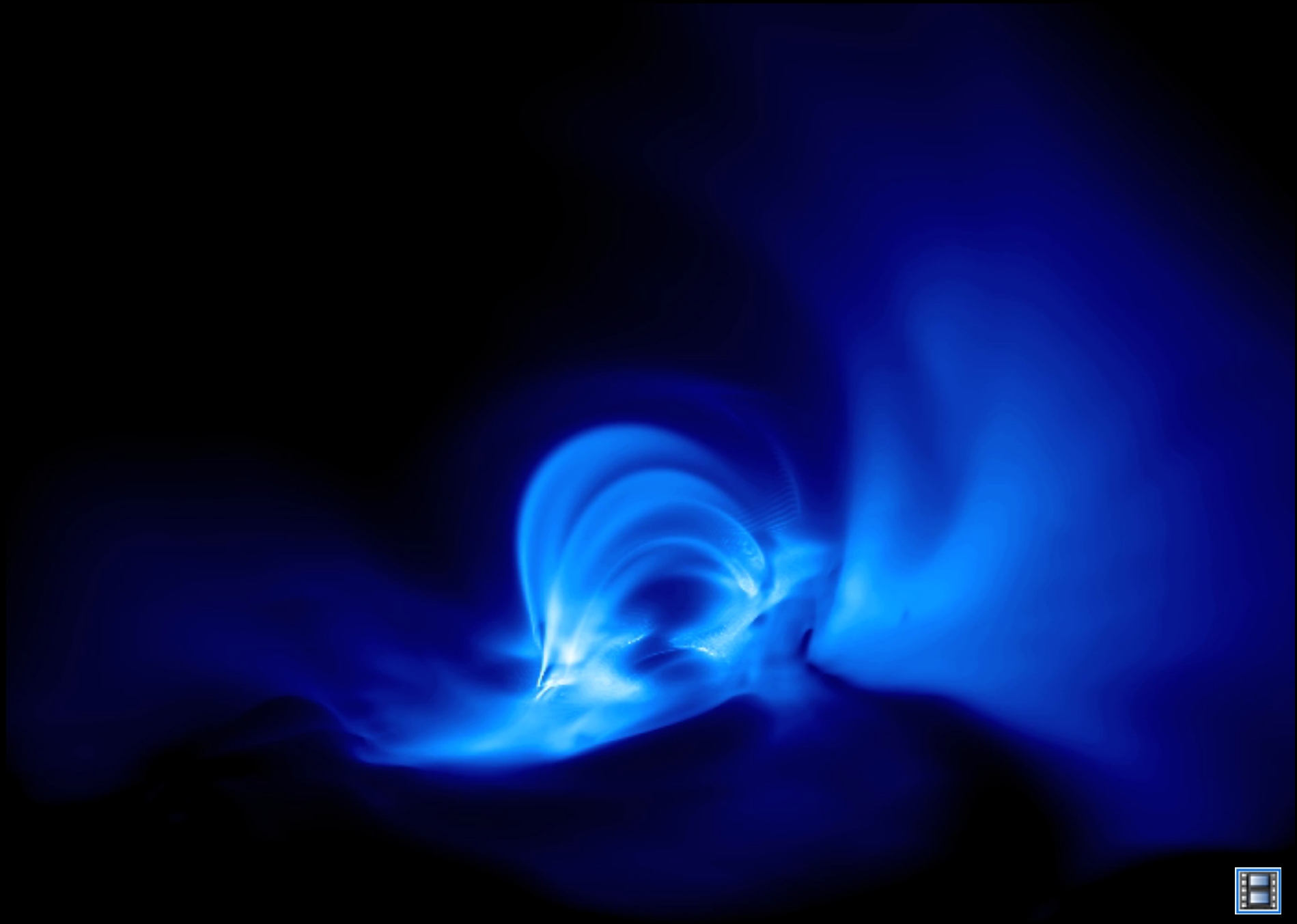

Case 979

Observed EUV (SOHO/EIT) and X-Ray (Yohkoh/SXT) Emission on August 30, 1996 [Log_{10}DN/s]

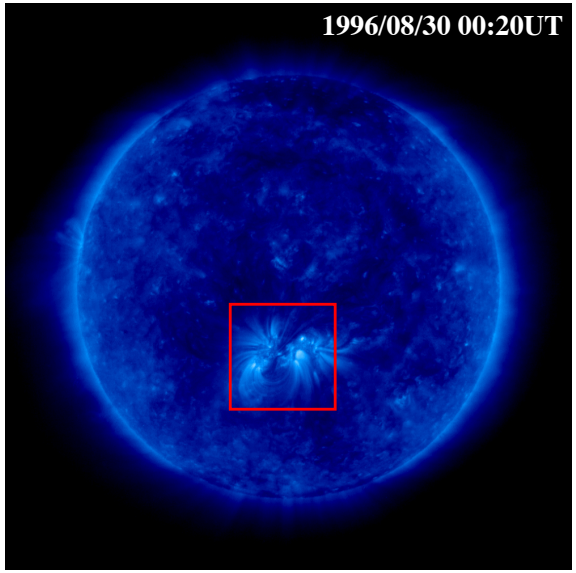

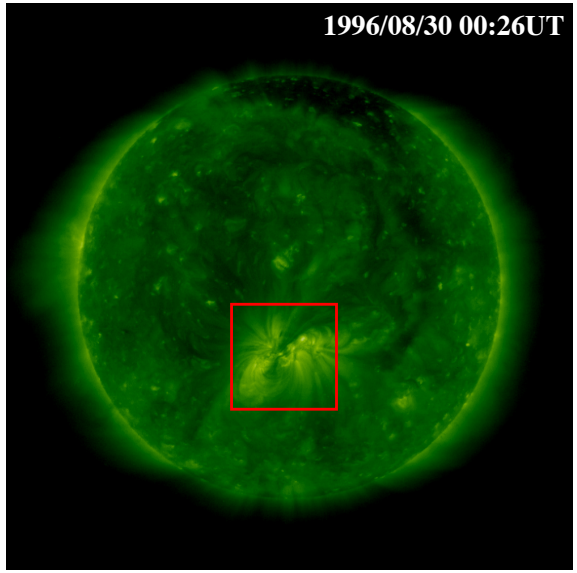

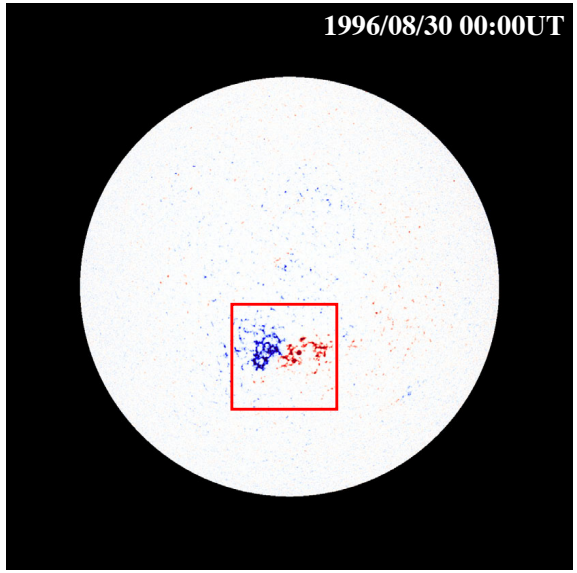

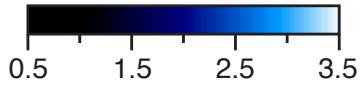

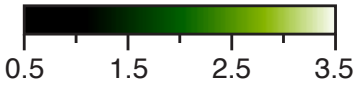

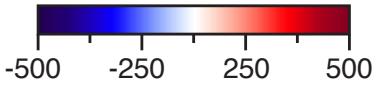

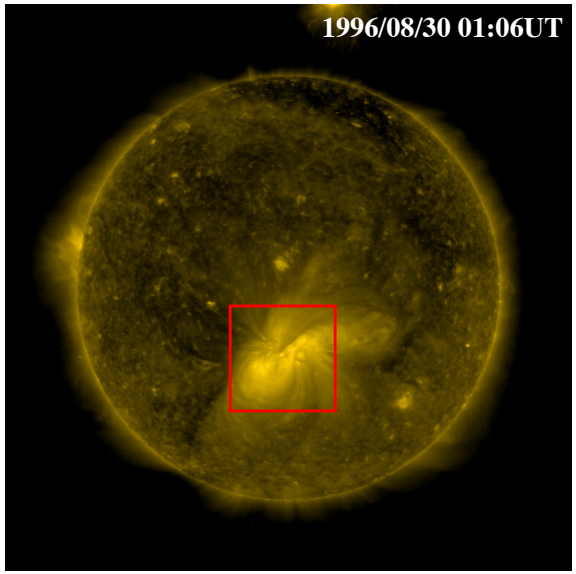

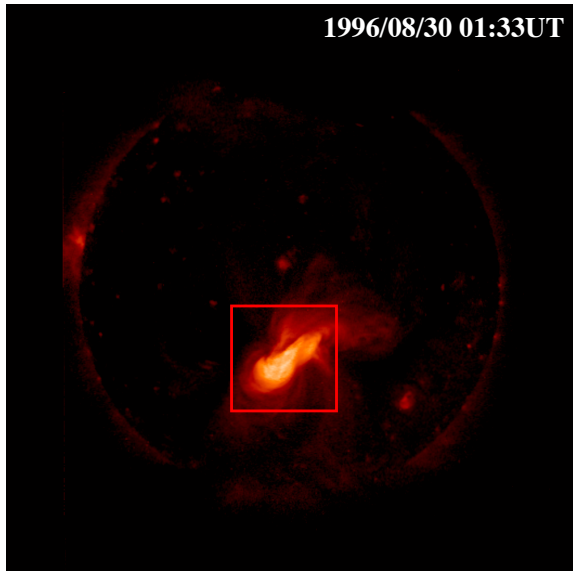

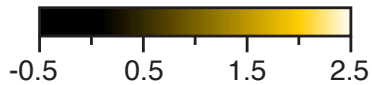

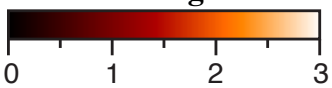

Comparing Observed EUV and X-Ray Emission on August 30, 1996 with Simulated Emission from a 3D MHD Model

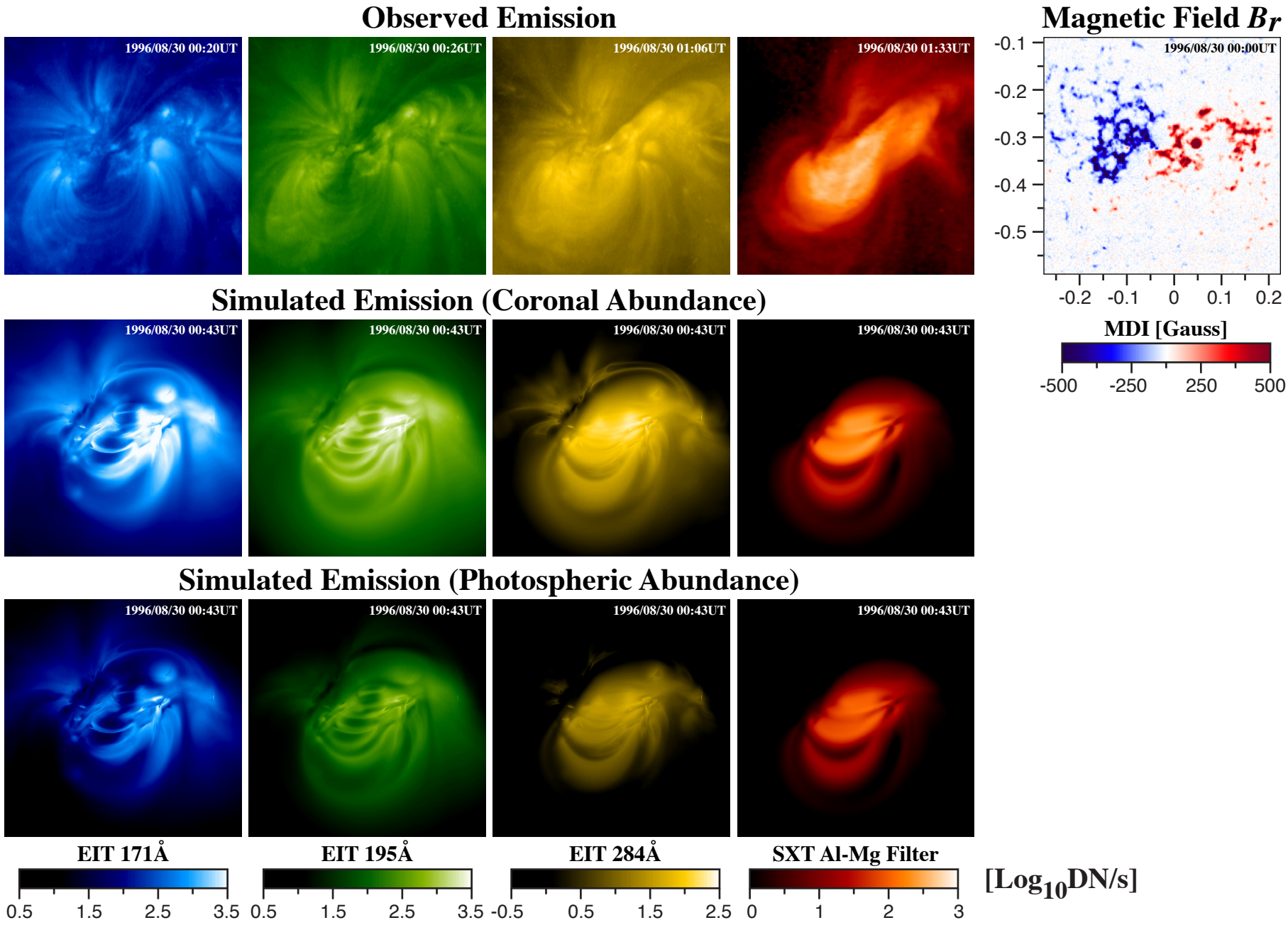

Field Line from a 3D Active Region Simulation

NLFFF Model of AR 7986, August 1996

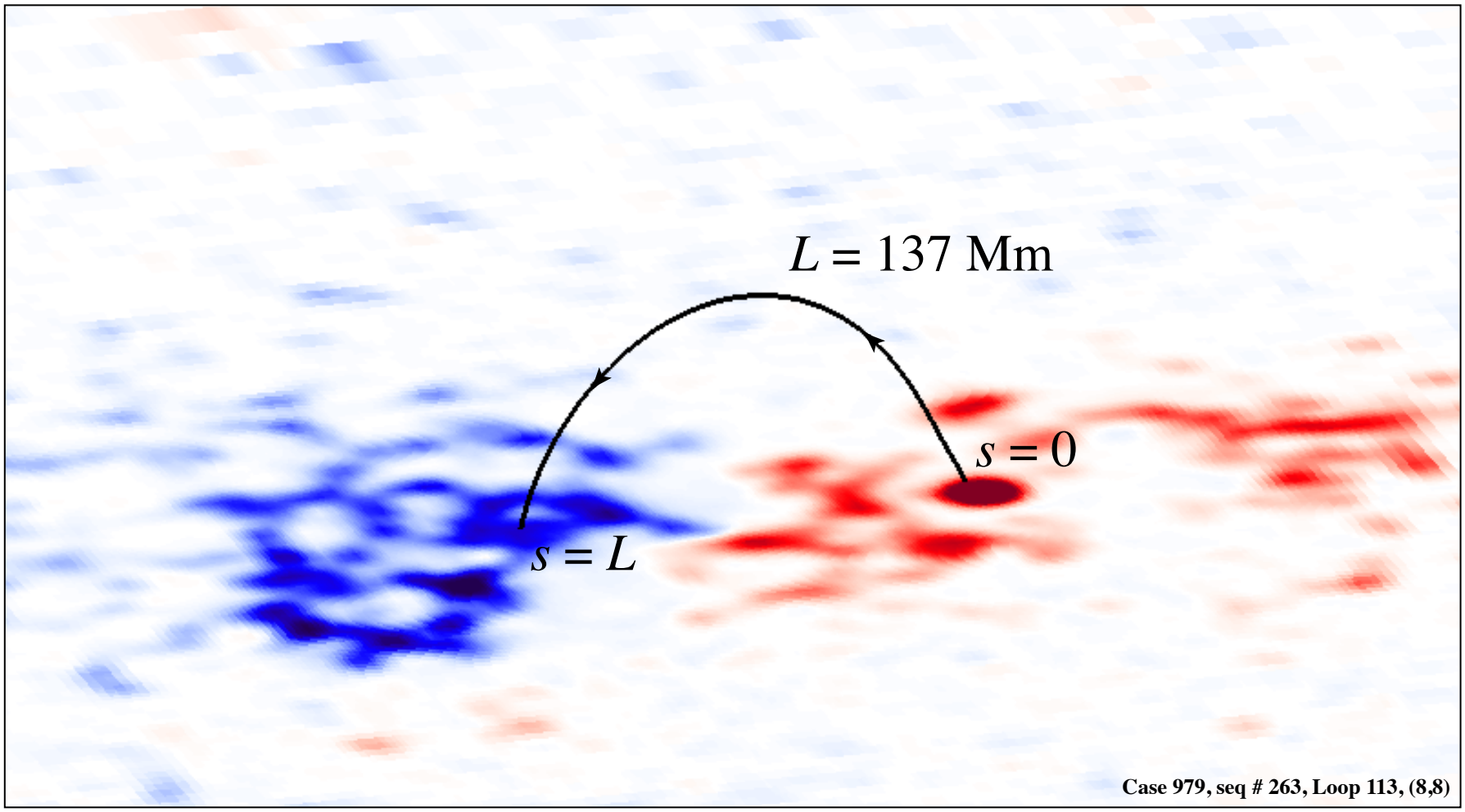

Field Line from AR7986 Simulation

Magnetic Field Strength

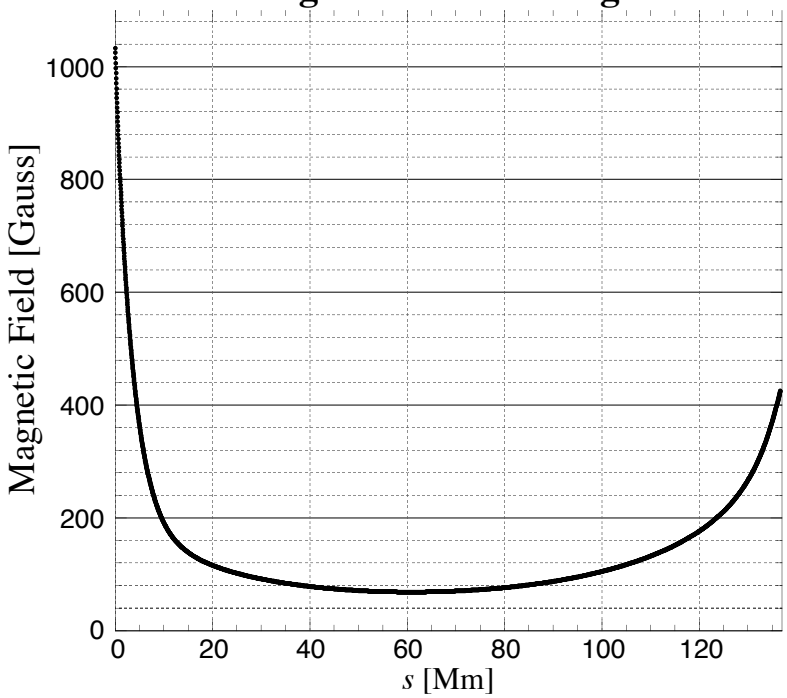

Loop Cross-Sectional Area

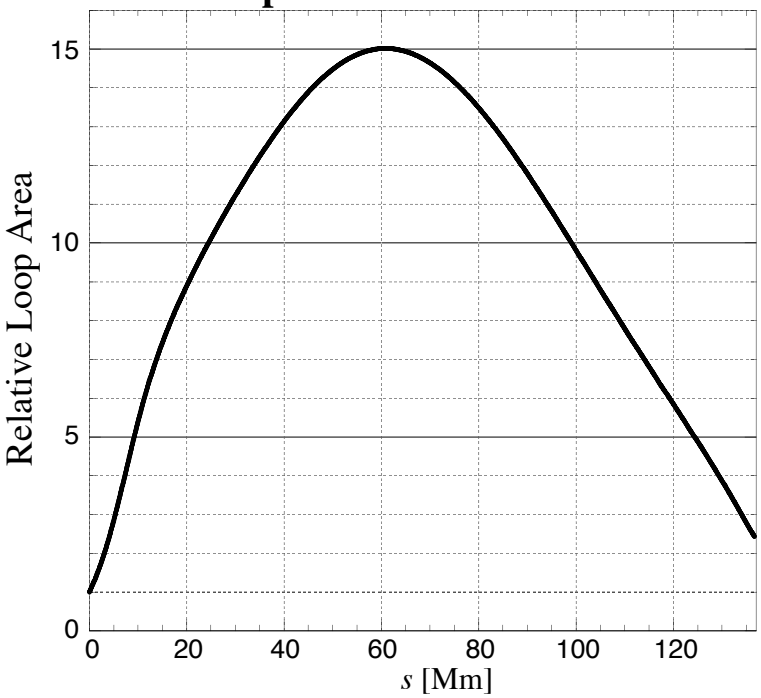

Heating Profile

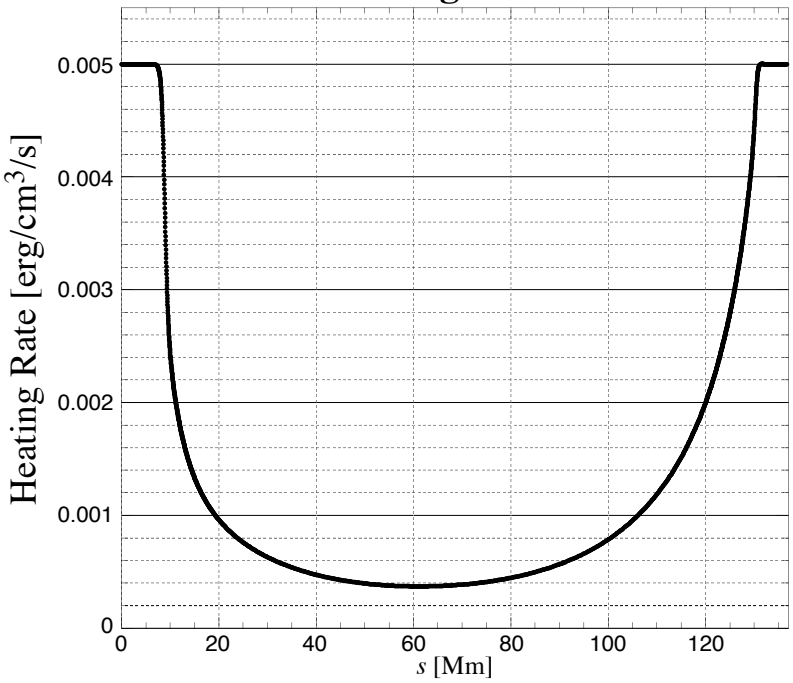

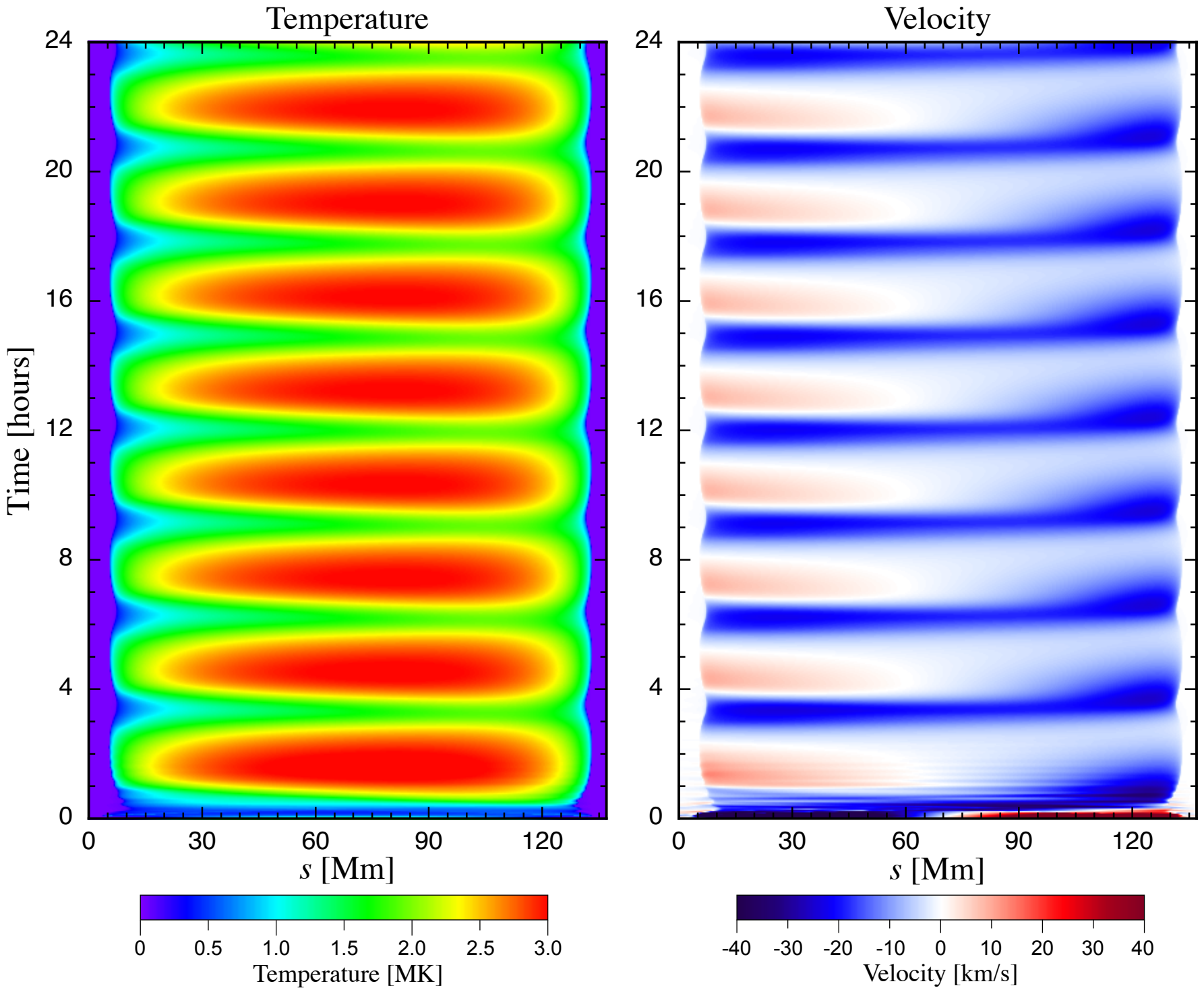
Solution Along a Magnetic Field Line from AR 7986 (August 1996)
Temperature
Velocity
Time [hours]
0
4
8
12
16
20
24
0
30
60
90
120
s [Mm]
0
0.5
1.0
1.5
2.0
2.5
3.0
Temperature [MK]
-40
-30
-20
-10
0
10
20
30
40
Velocity [km/s]

INCOMPLETE CONDENSATION
Loop from AR7986 (Case11)

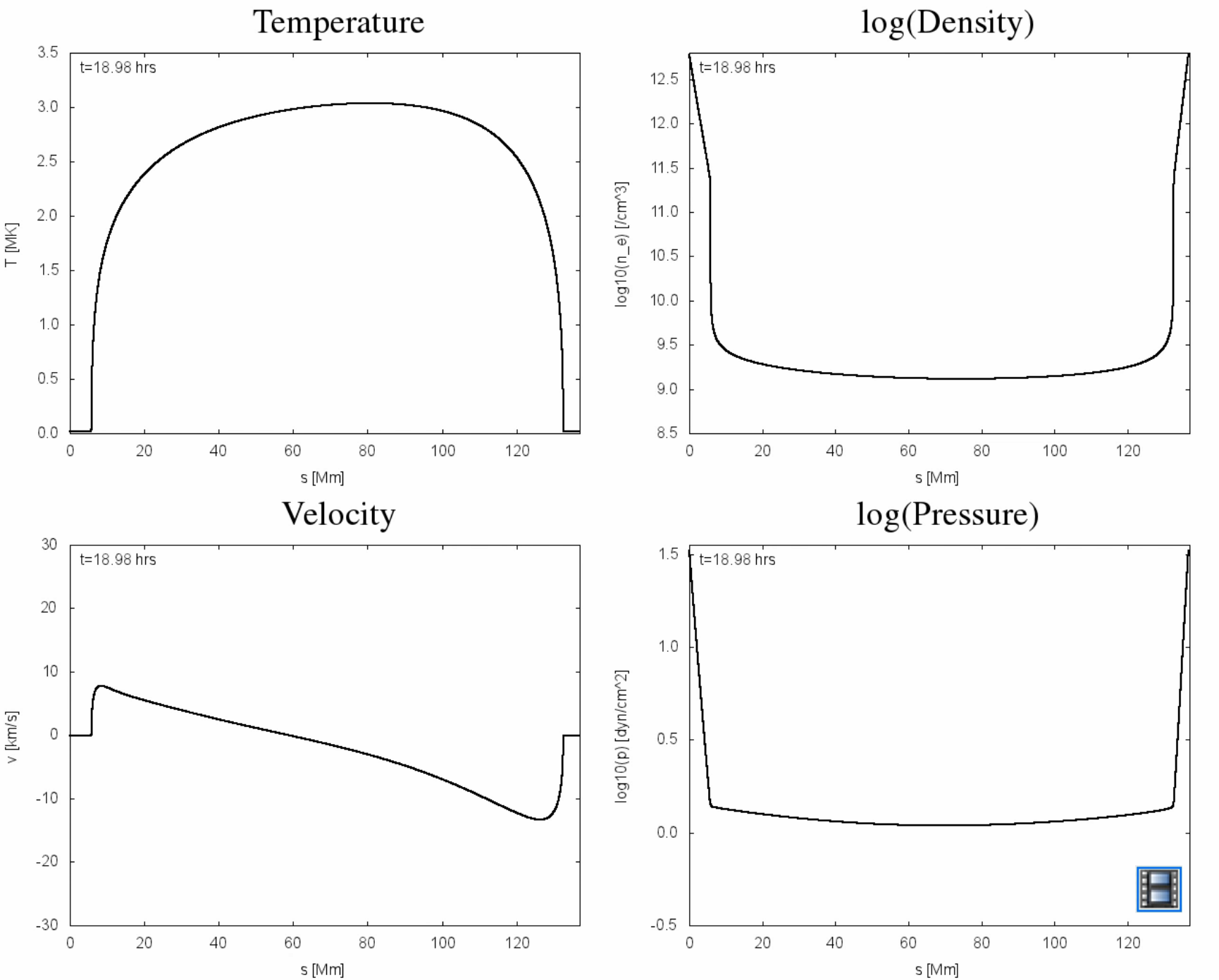

Emission From the Loop (for $ds = 10^9$ cm)

Loop from 3D AR Simulation: Case 979, seq # 263, Loop 113, (8,8)

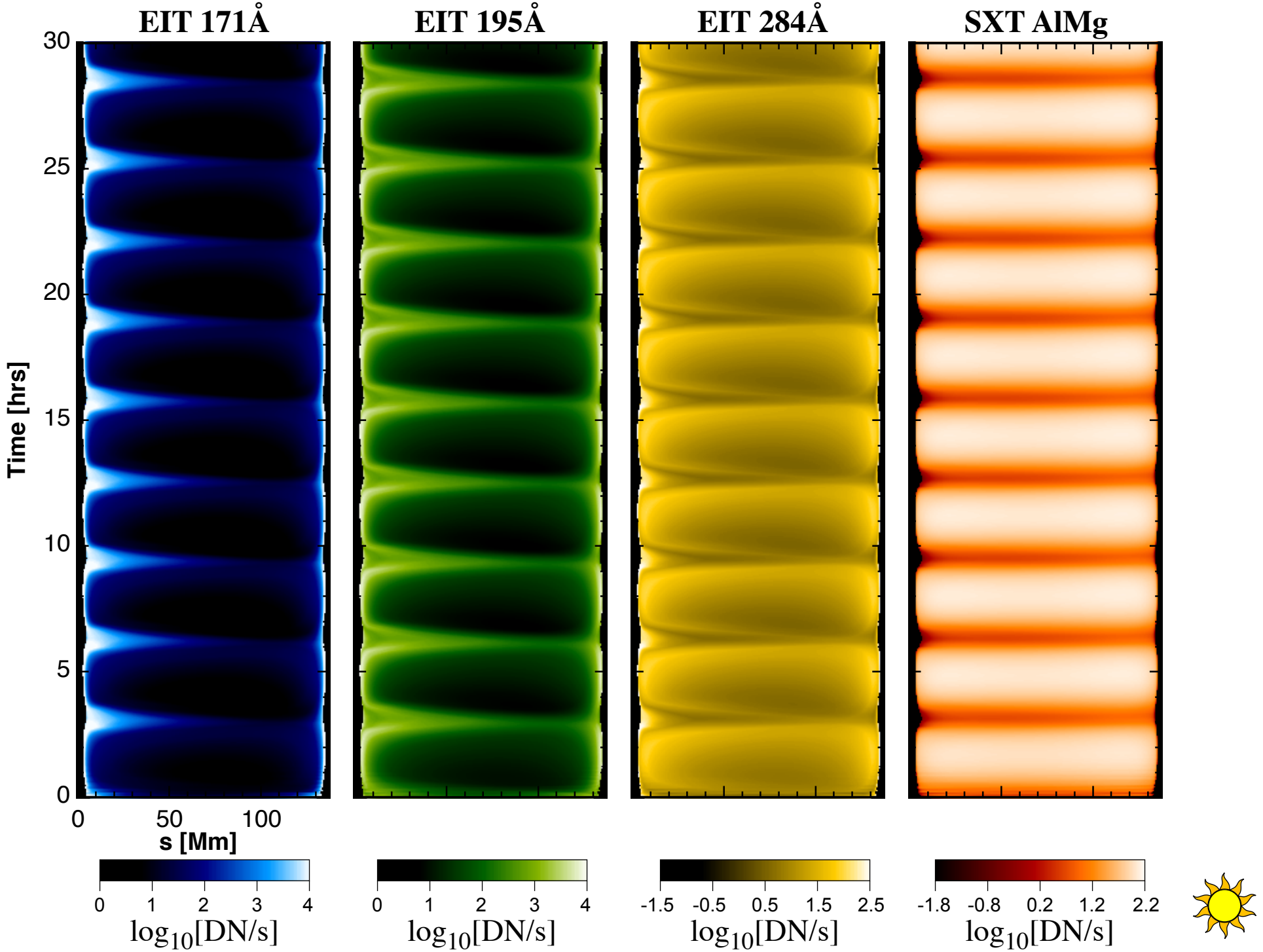

Delays Between Filters

Loop from 3D AR Simulation: Case 979, seq # 263, Loop 113, (8,8)

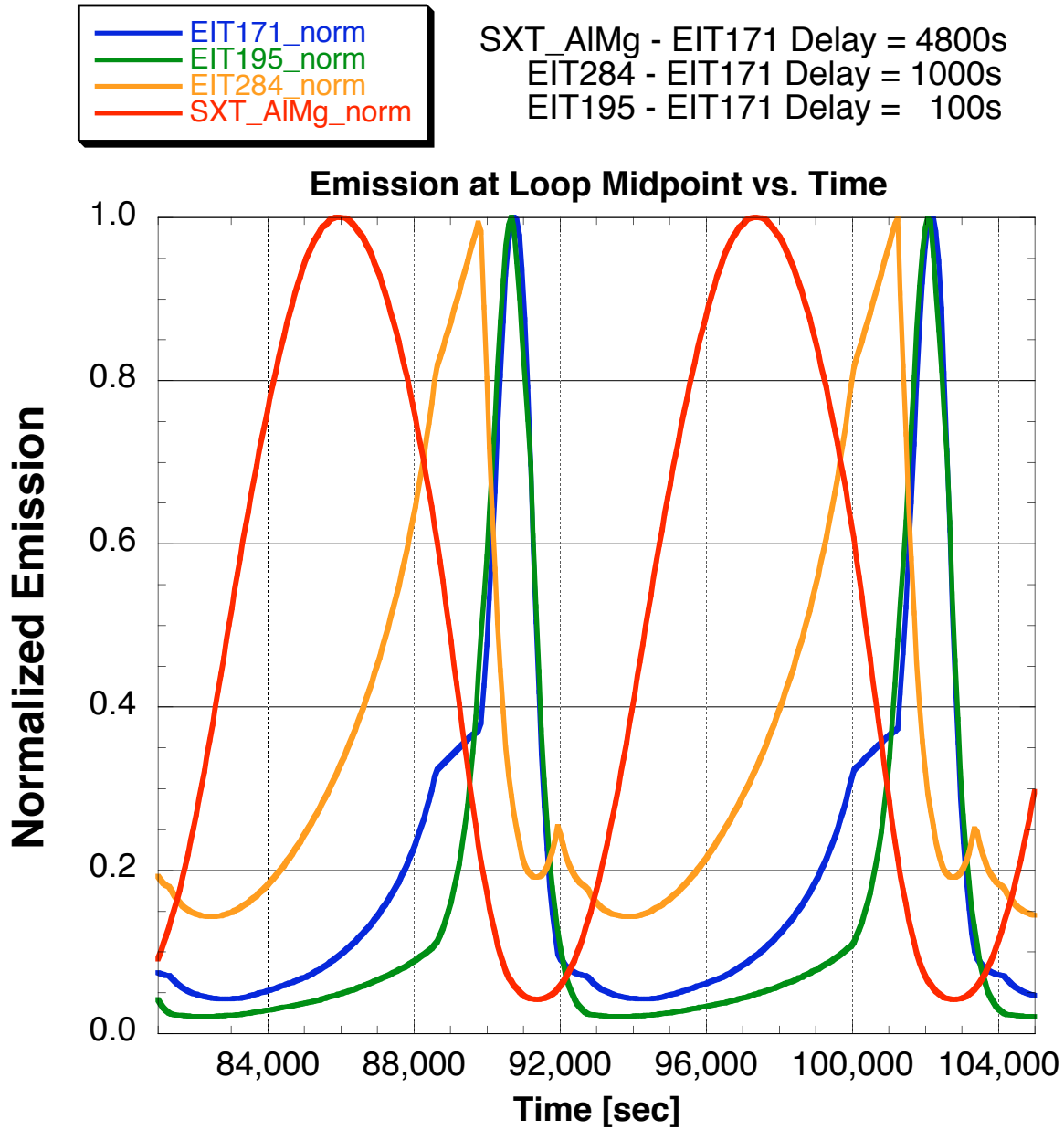

Bundle of 15 × 15 Magnetic Field Lines

($j = 1, 2, ..., 15$ and $k = 1, 2, ..., 15$)

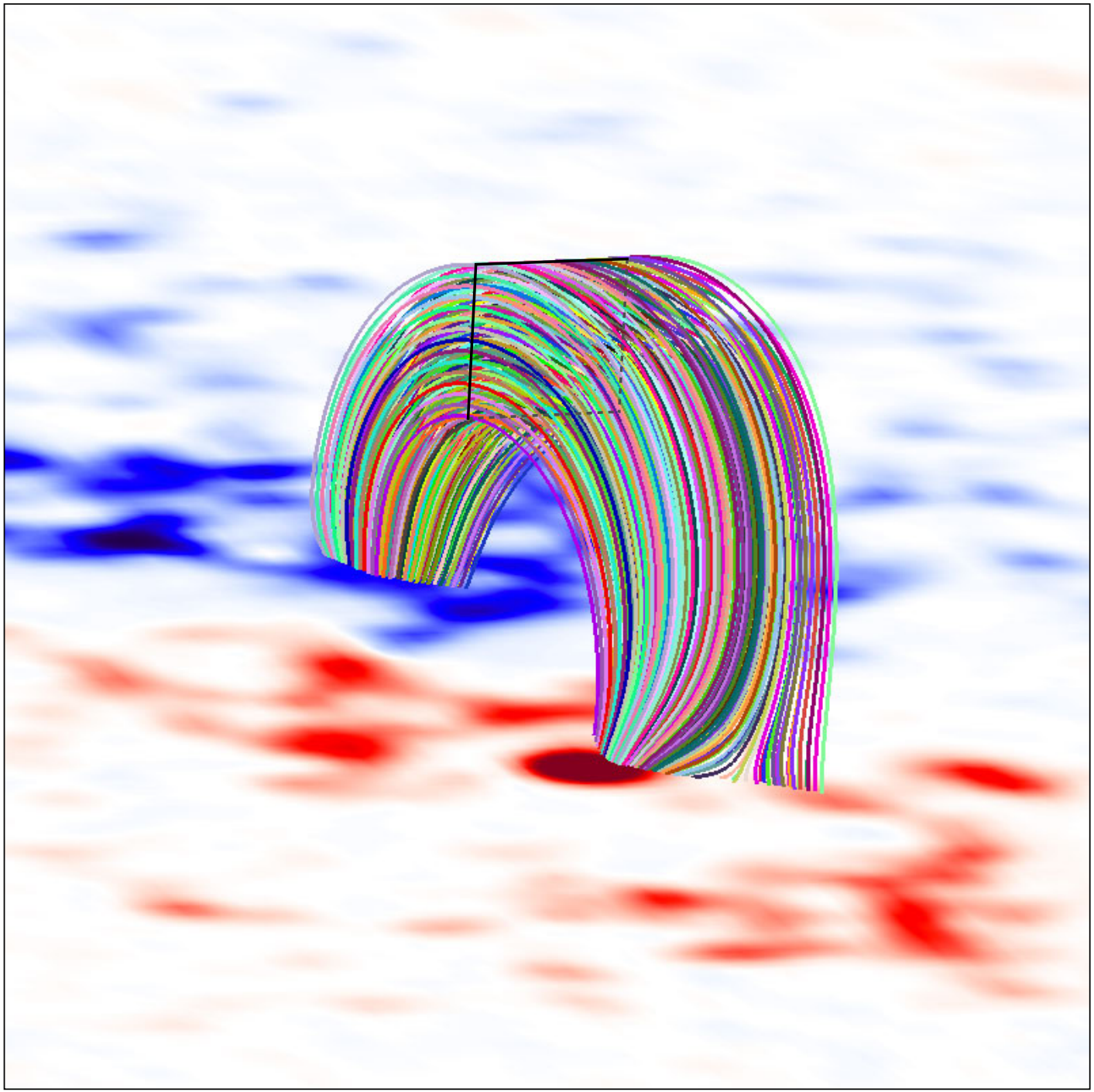

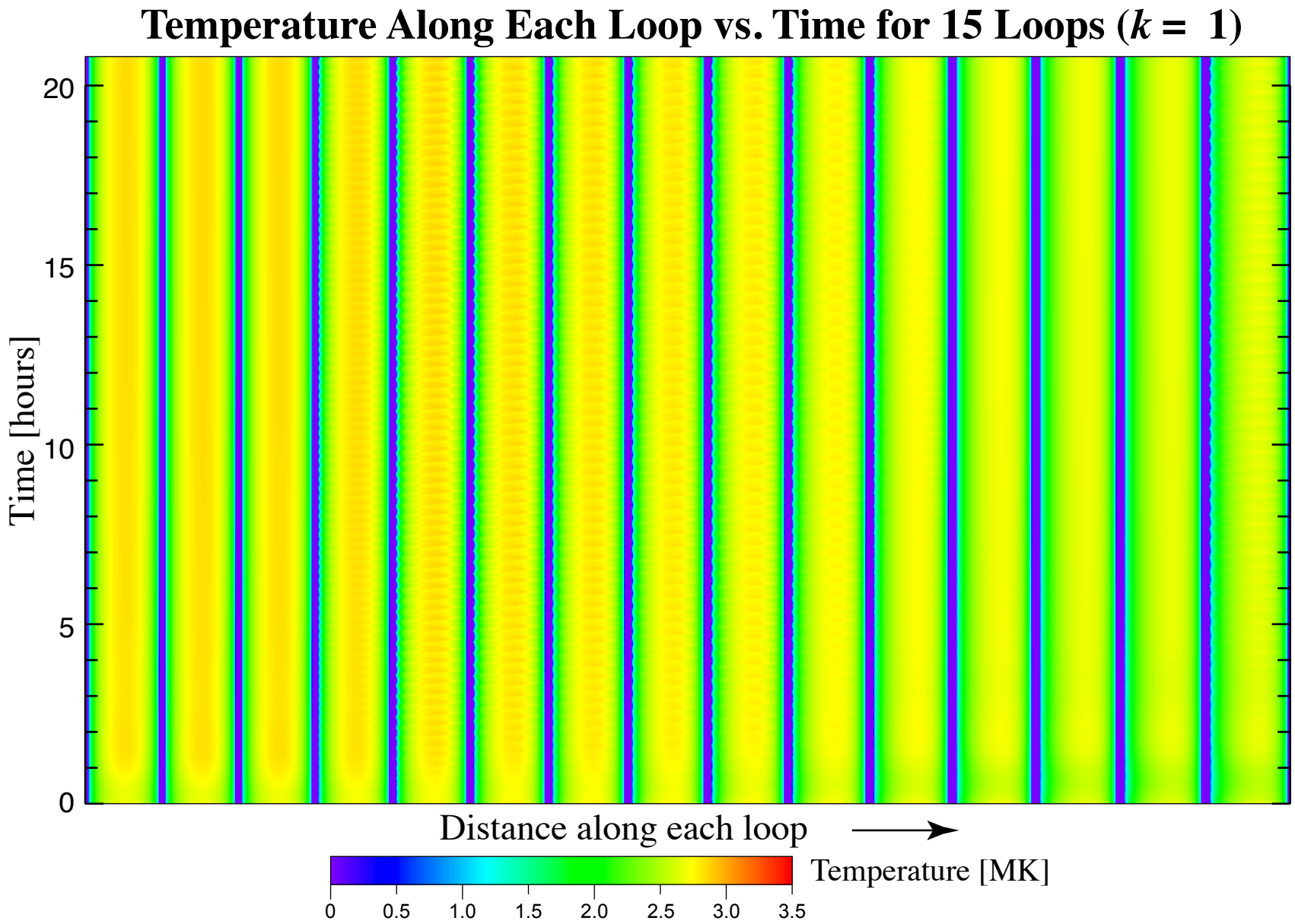
Temperature Along Each Loop vs. Time for 15 Loops (k = 1)
Time [hours]
0
5
10
15
20
Distance along each loop
Temperature [MK]
0
0.5
1.0
1.5
2.0
2.5
3.0
3.5

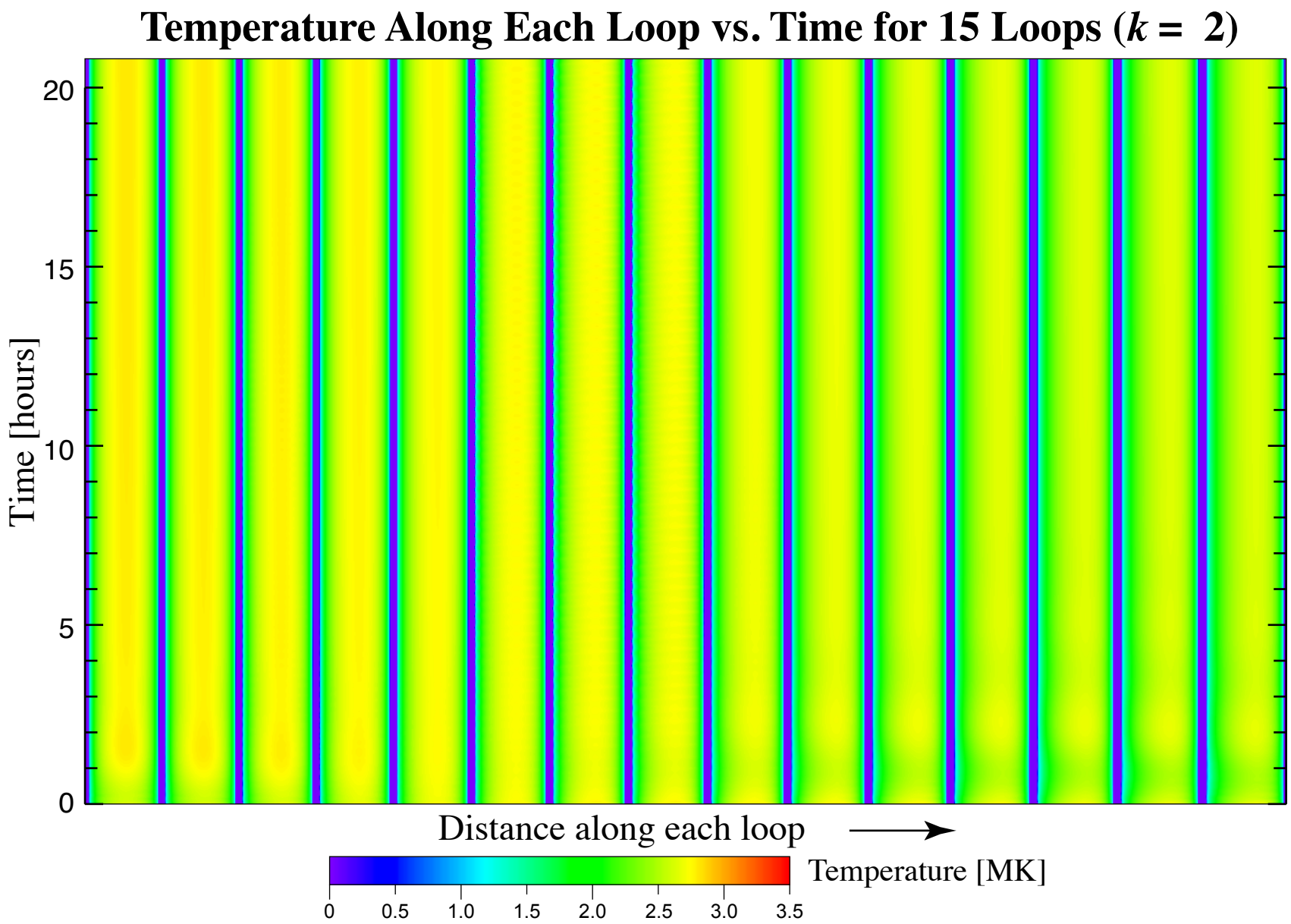
Temperature Along Each Loop vs. Time for 15 Loops (k = 2)
Time [hours]
0
5
10
15
20
Distance along each loop
Temperature [MK]
0
0.5
1.0
1.5
2.0
2.5
3.0
3.5

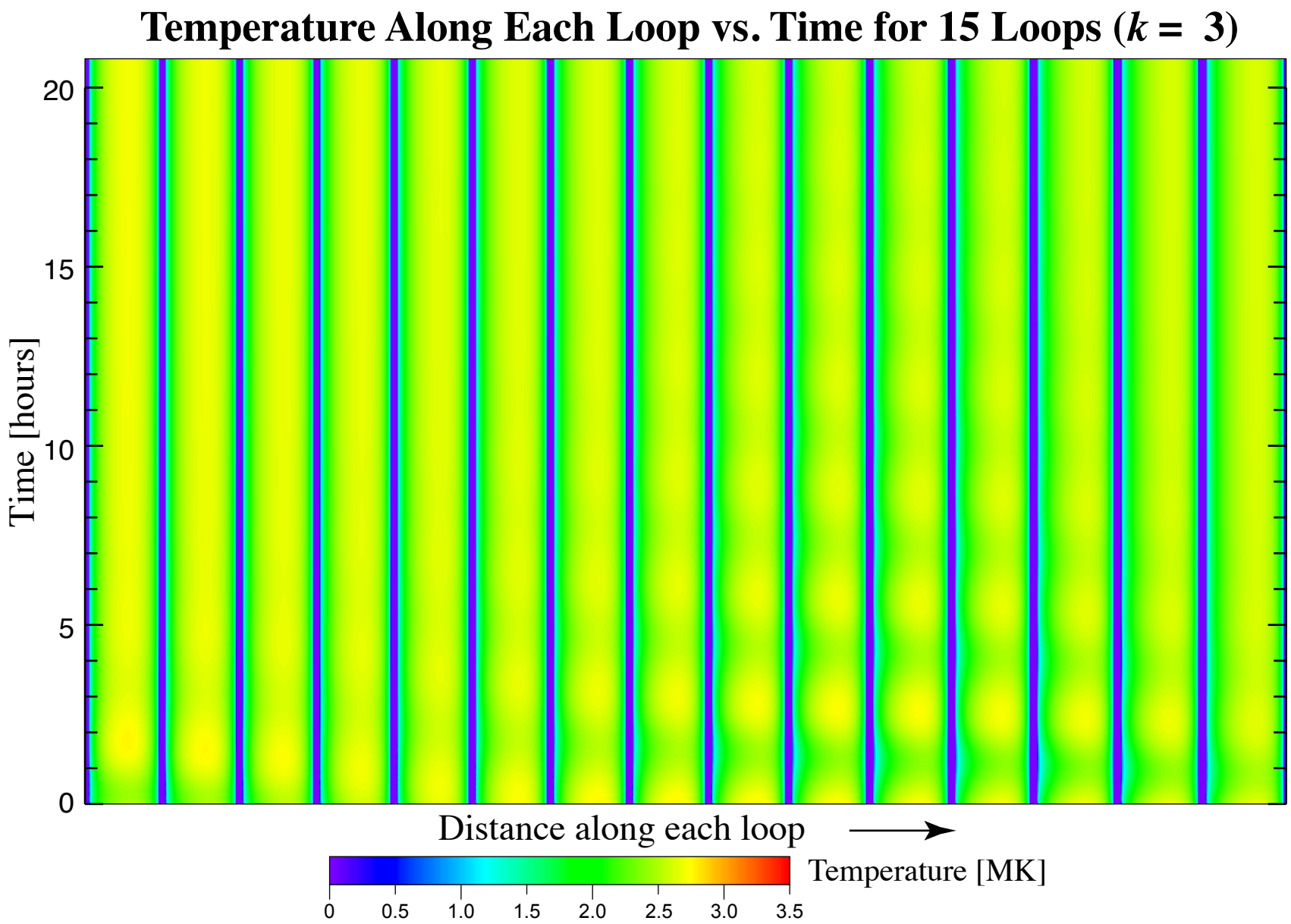
Temperature Along Each Loop vs. Time for 15 Loops (k = 3)
Time [hours]
0
5
10
15
20
Distance along each loop
Temperature [MK]
0
0.5
1.0
1.5
2.0
2.5
3.0
3.5

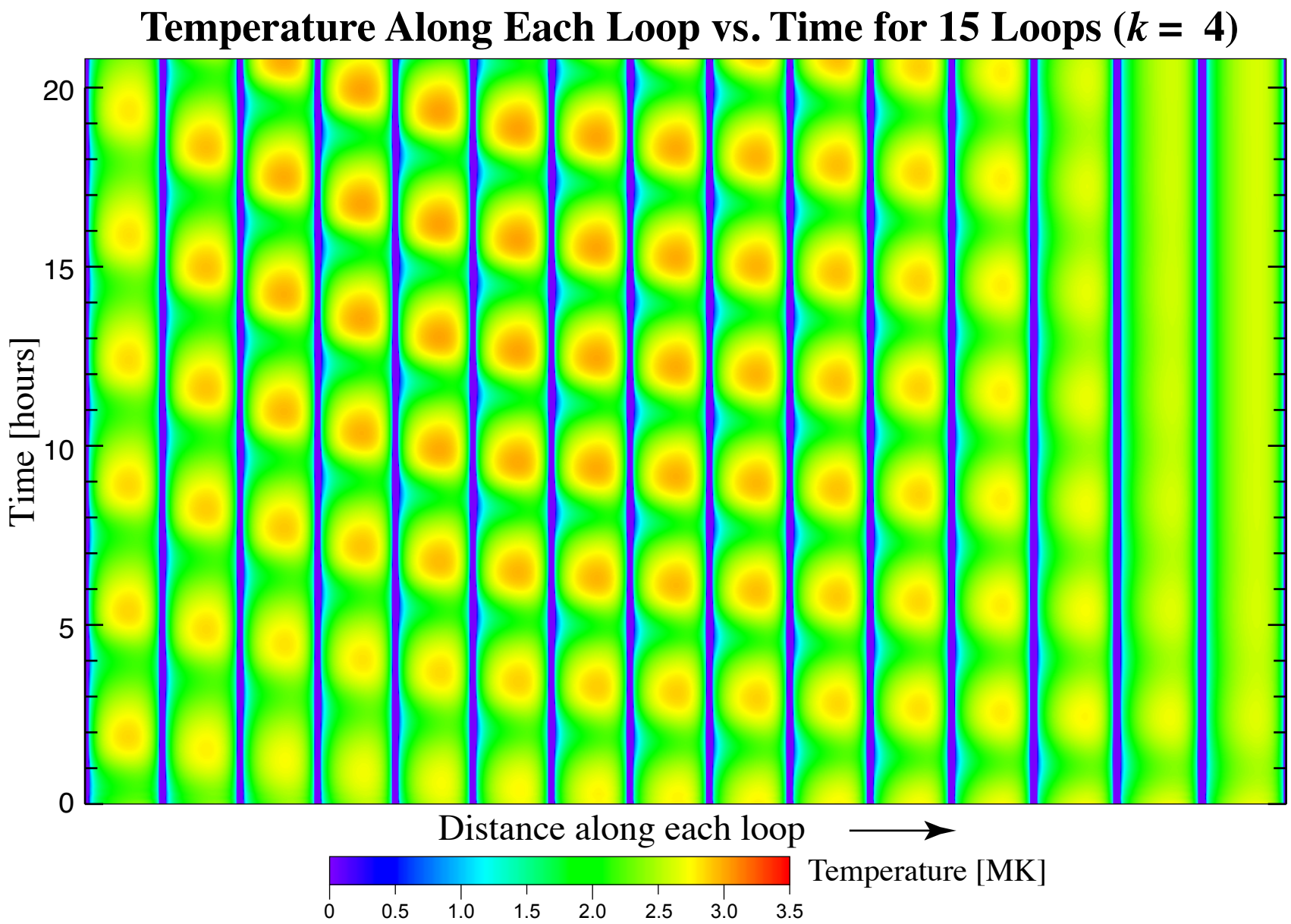
Temperature Along Each Loop vs. Time for 15 Loops (k = 4)
Time [hours]
0
5
10
15
20
Distance along each loop
Temperature [MK]
0
0.5
1.0
1.5
2.0
2.5
3.0
3.5

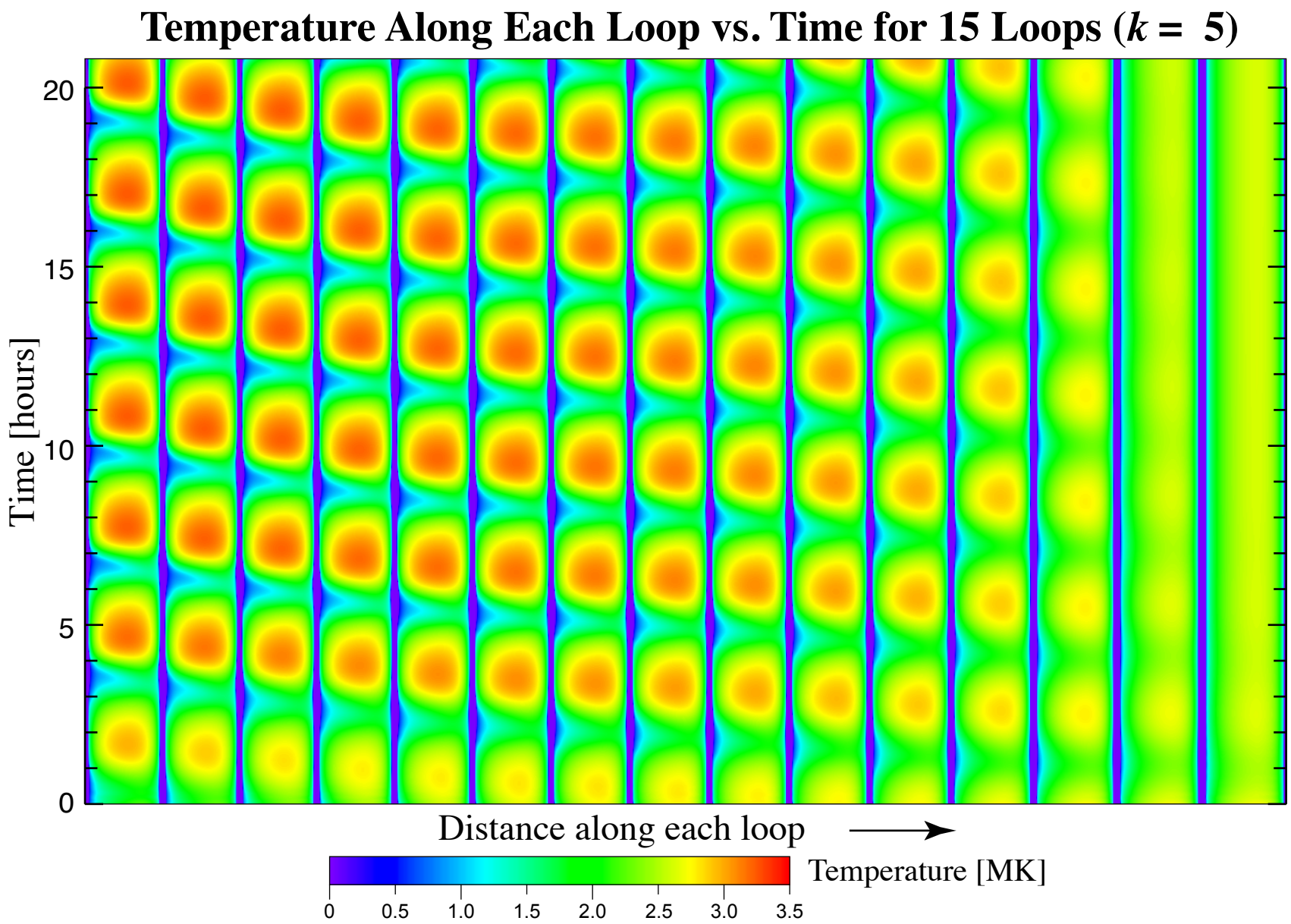
Temperature Along Each Loop vs. Time for 15 Loops (k = 5)
Time [hours]
0
5
10
15
20
Distance along each loop
Temperature [MK]
0
0.5
1.0
1.5
2.0
2.5
3.0
3.5

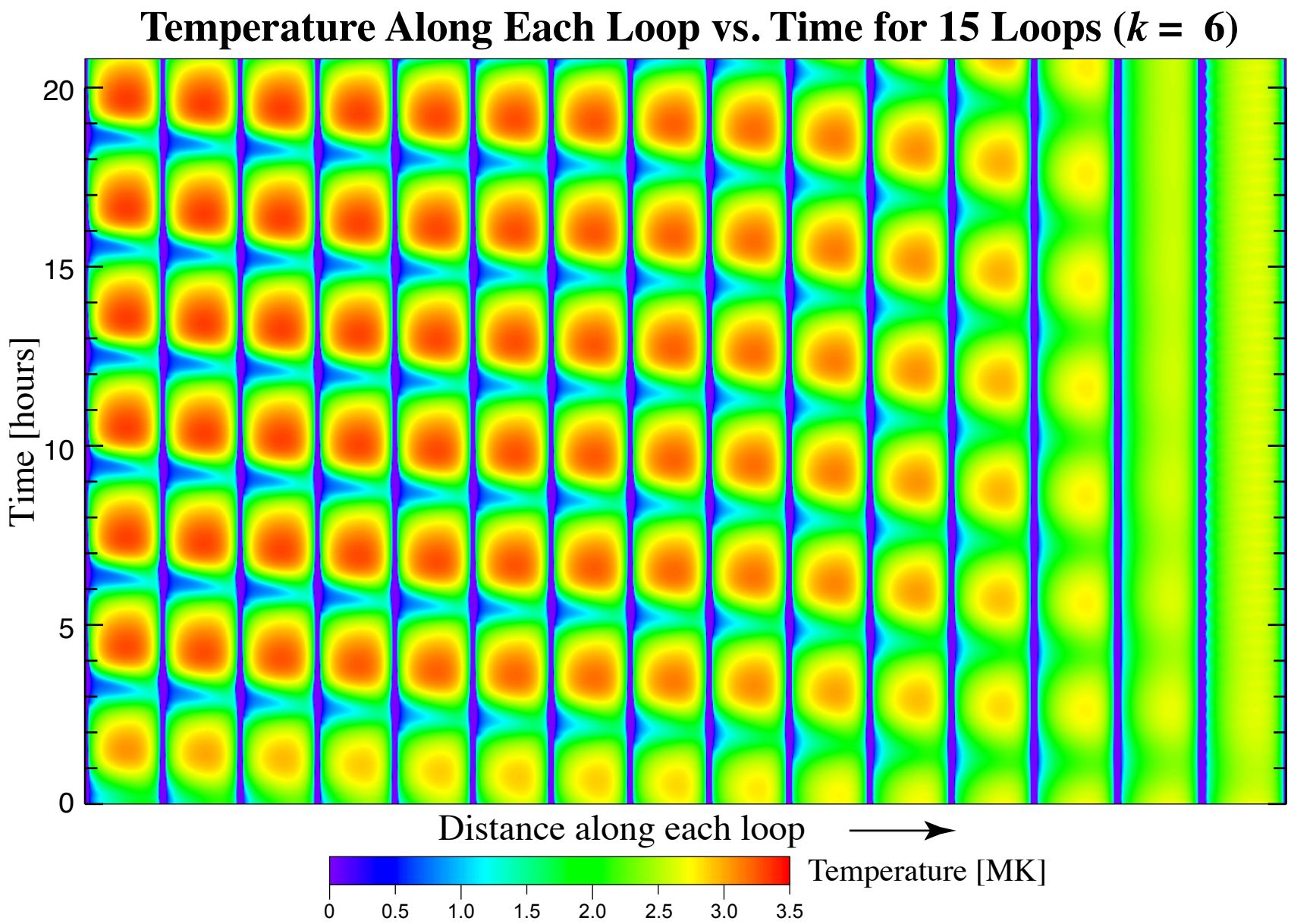
Temperature Along Each Loop vs. Time for 15 Loops (k = 6)
Time [hours]
0
5
10
15
20
Distance along each loop
Temperature [MK]
0
0.5
1.0
1.5
2.0
2.5
3.0
3.5

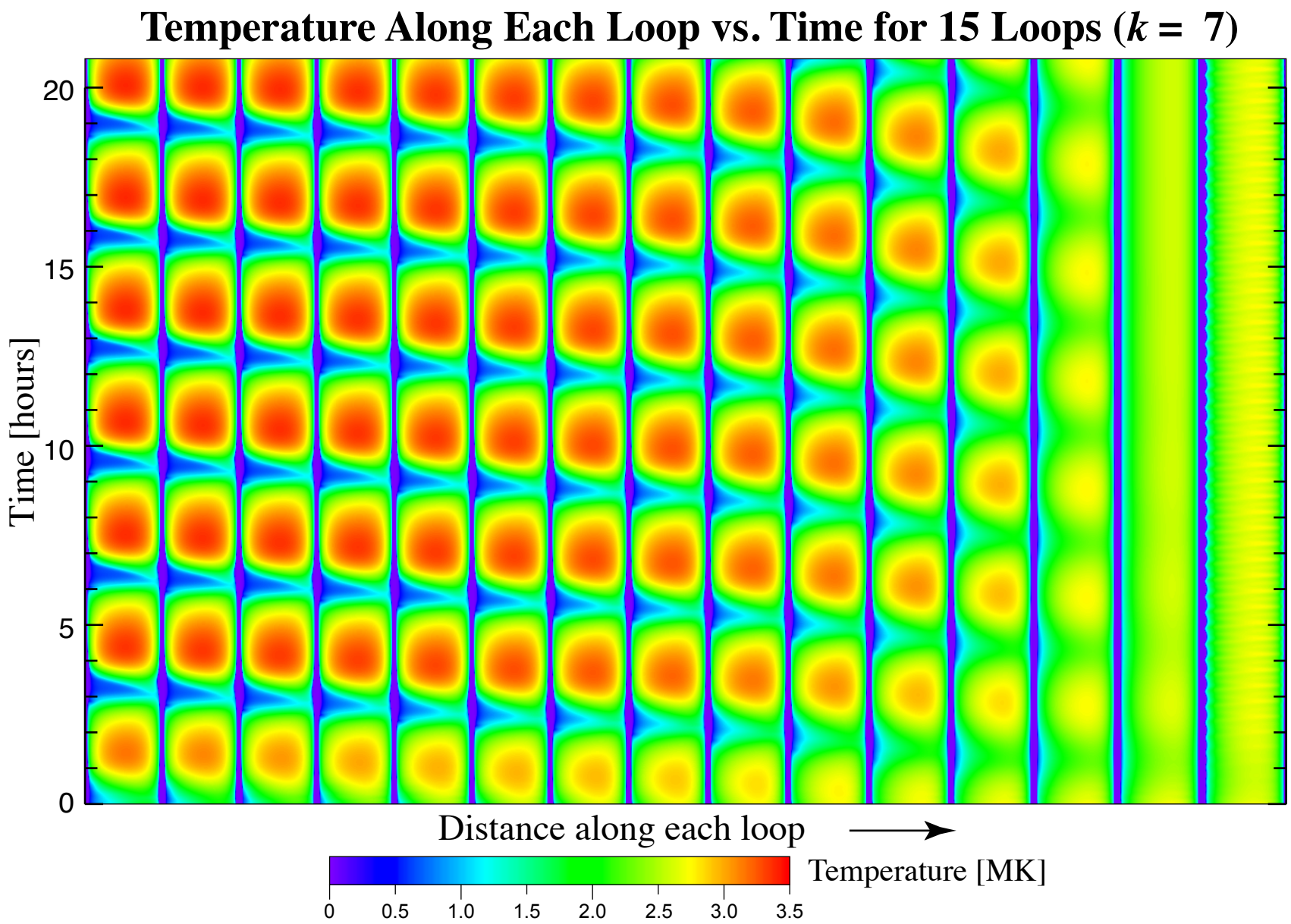
Temperature Along Each Loop vs. Time for 15 Loops (k = 7)
Time [hours]
0
5
10
15
20
Distance along each loop
Temperature [MK]
0
0.5
1.0
1.5
2.0
2.5
3.0
3.5

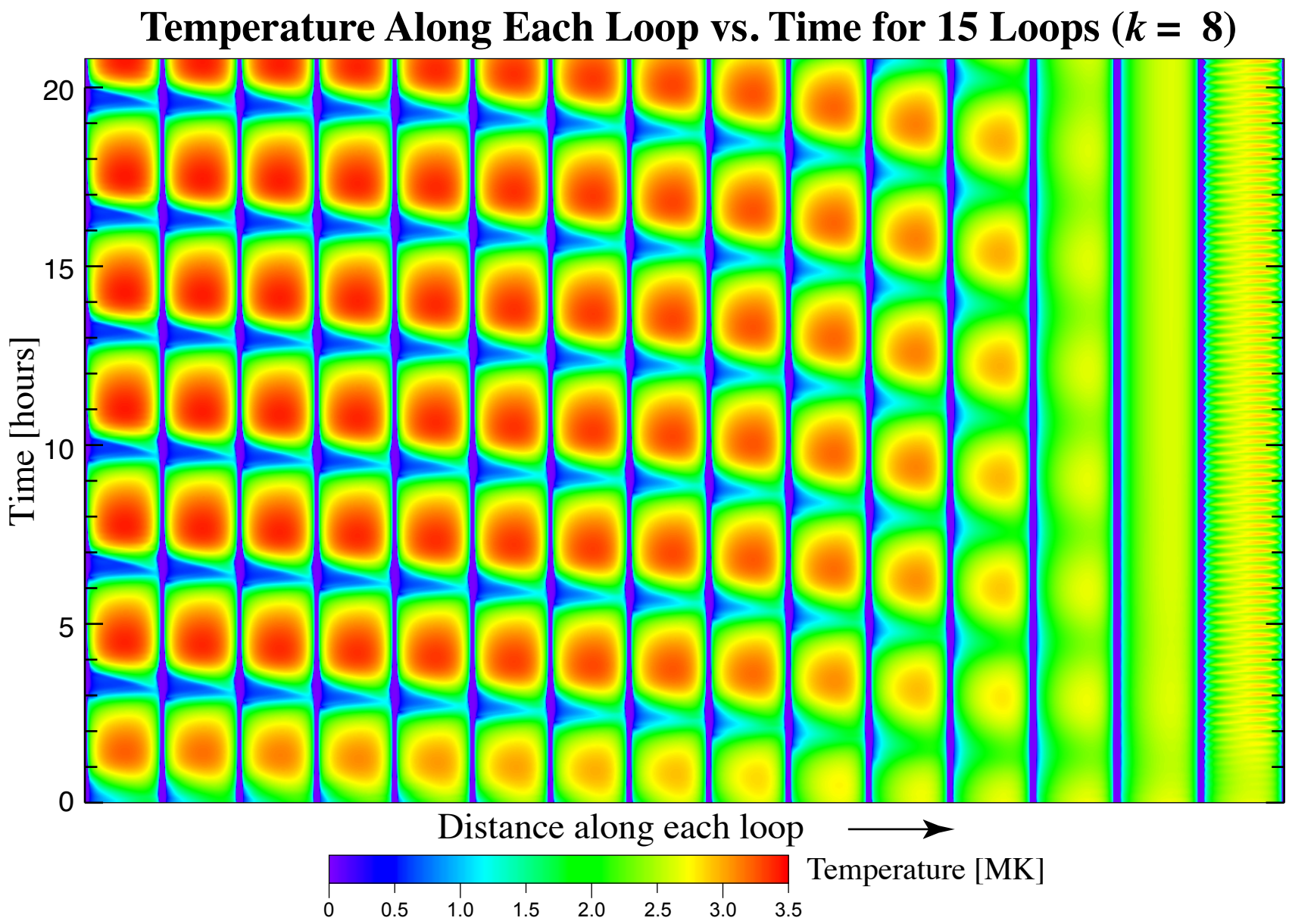
Temperature Along Each Loop vs. Time for 15 Loops (k = 8)
Time [hours]
0
5
10
15
20
Distance along each loop
Temperature [MK]
0
0.5
1.0
1.5
2.0
2.5
3.0
3.5

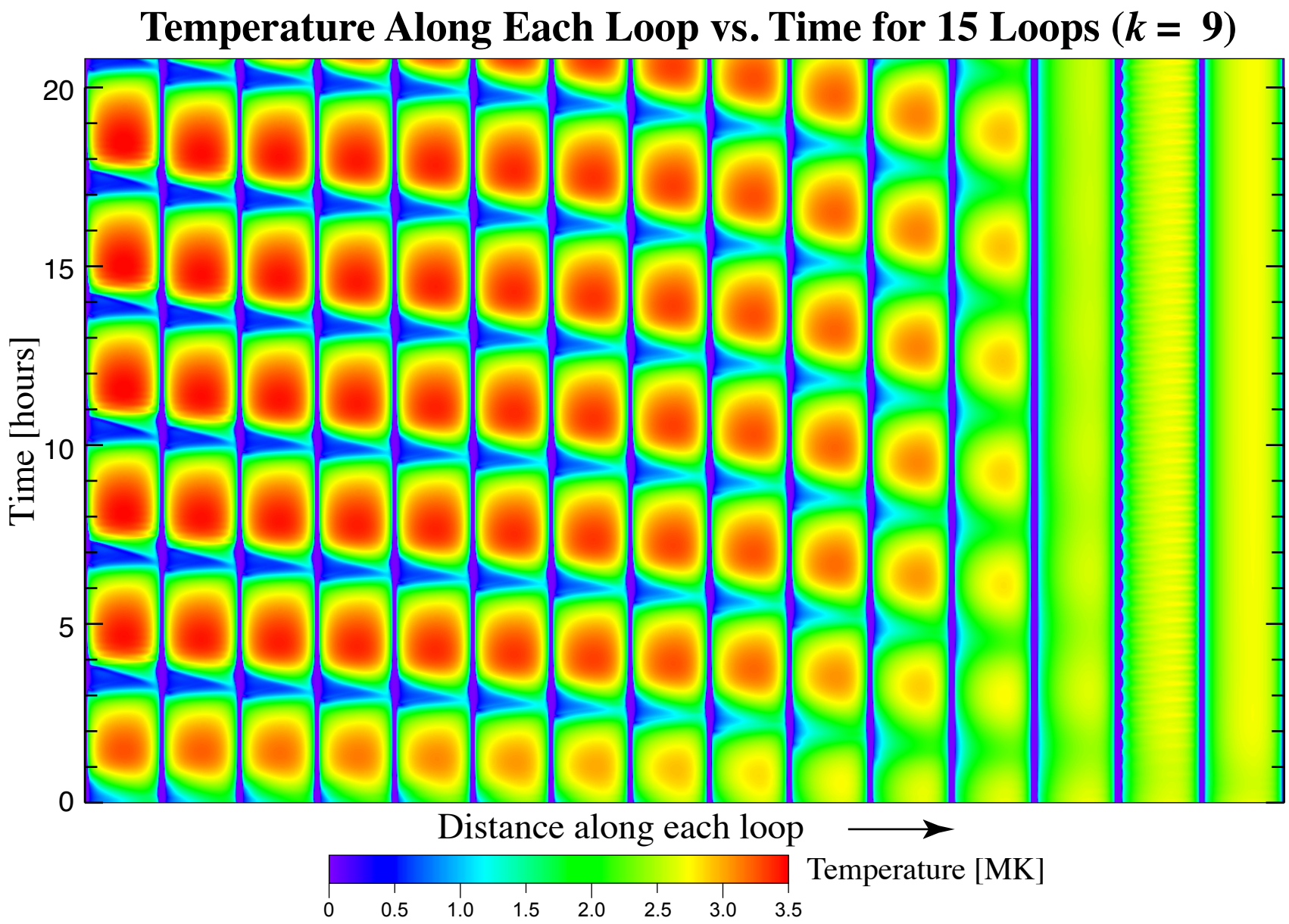
Temperature Along Each Loop vs. Time for 15 Loops (k = 9)
Time [hours]
0
5
10
15
20
Distance along each loop
Temperature [MK]
0
0.5
1.0
1.5
2.0
2.5
3.0
3.5

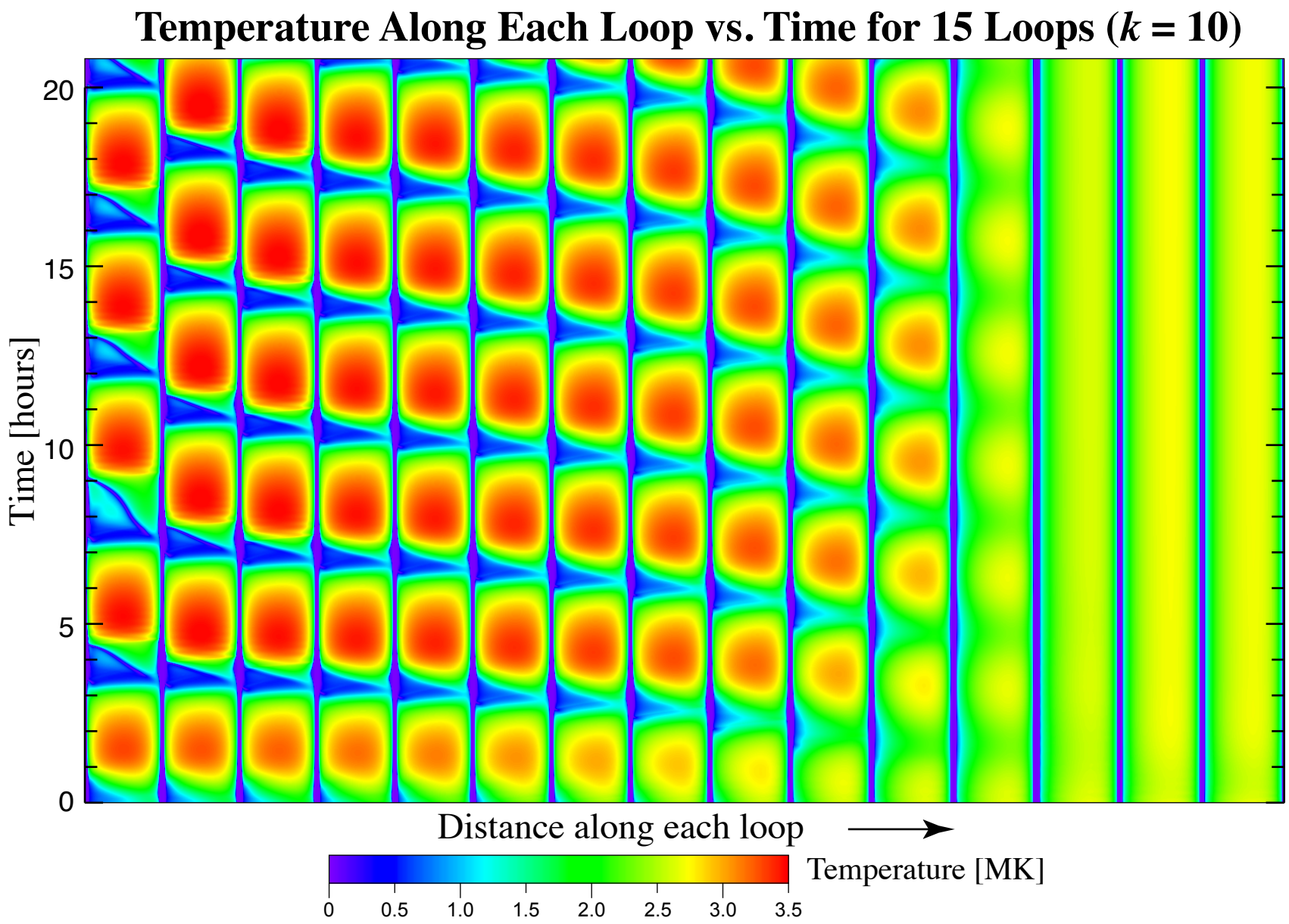
Temperature Along Each Loop vs. Time for 15 Loops (k = 10)
Time [hours]
0
5
10
15
20
Distance along each loop
Temperature [MK]
0
0.5
1.0
1.5
2.0
2.5
3.0
3.5

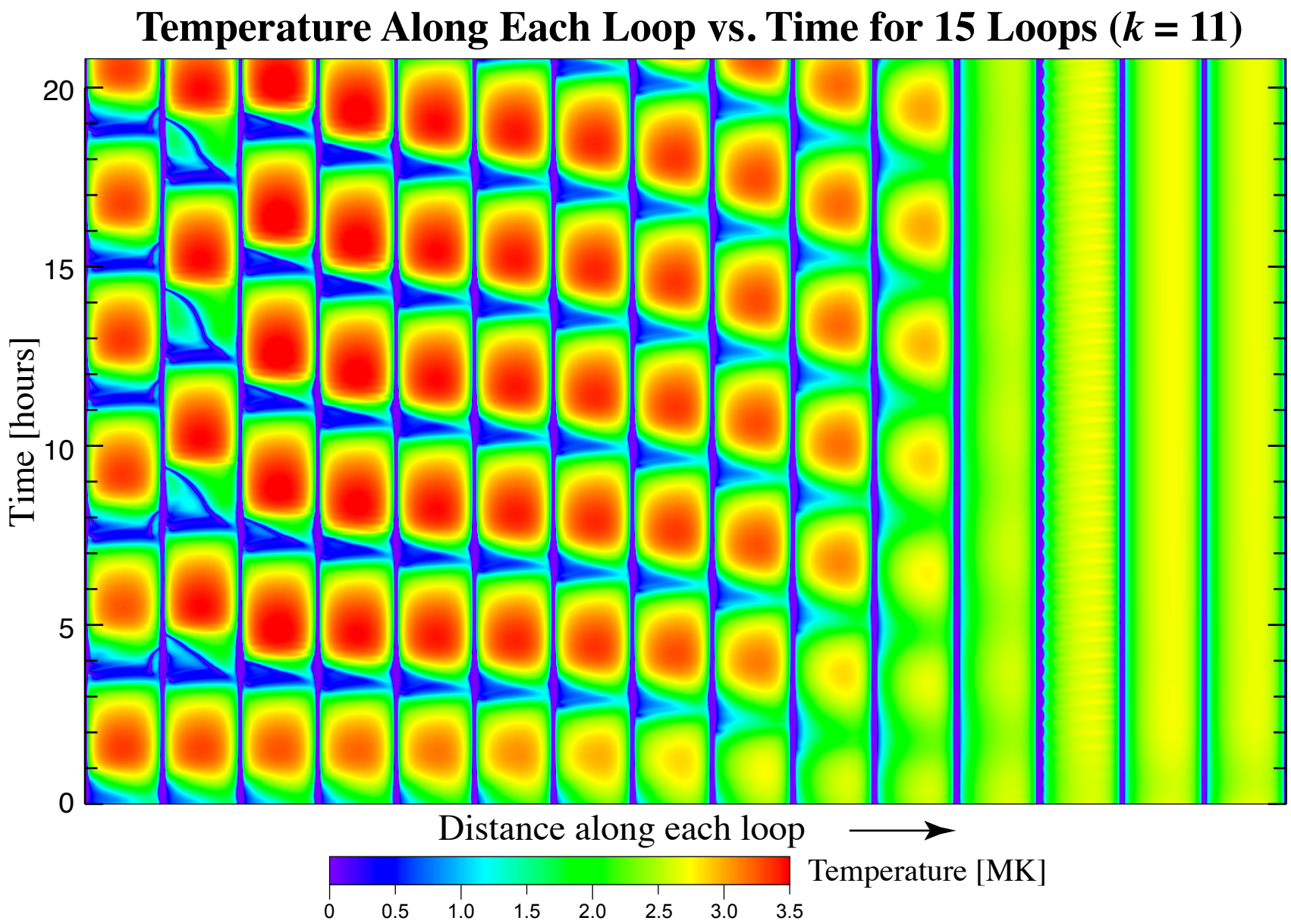
Temperature Along Each Loop vs. Time for 15 Loops (k = 11)
Time [hours]
0
5
10
15
20
Distance along each loop
Temperature [MK]
0
0.5
1.0
1.5
2.0
2.5
3.0
3.5

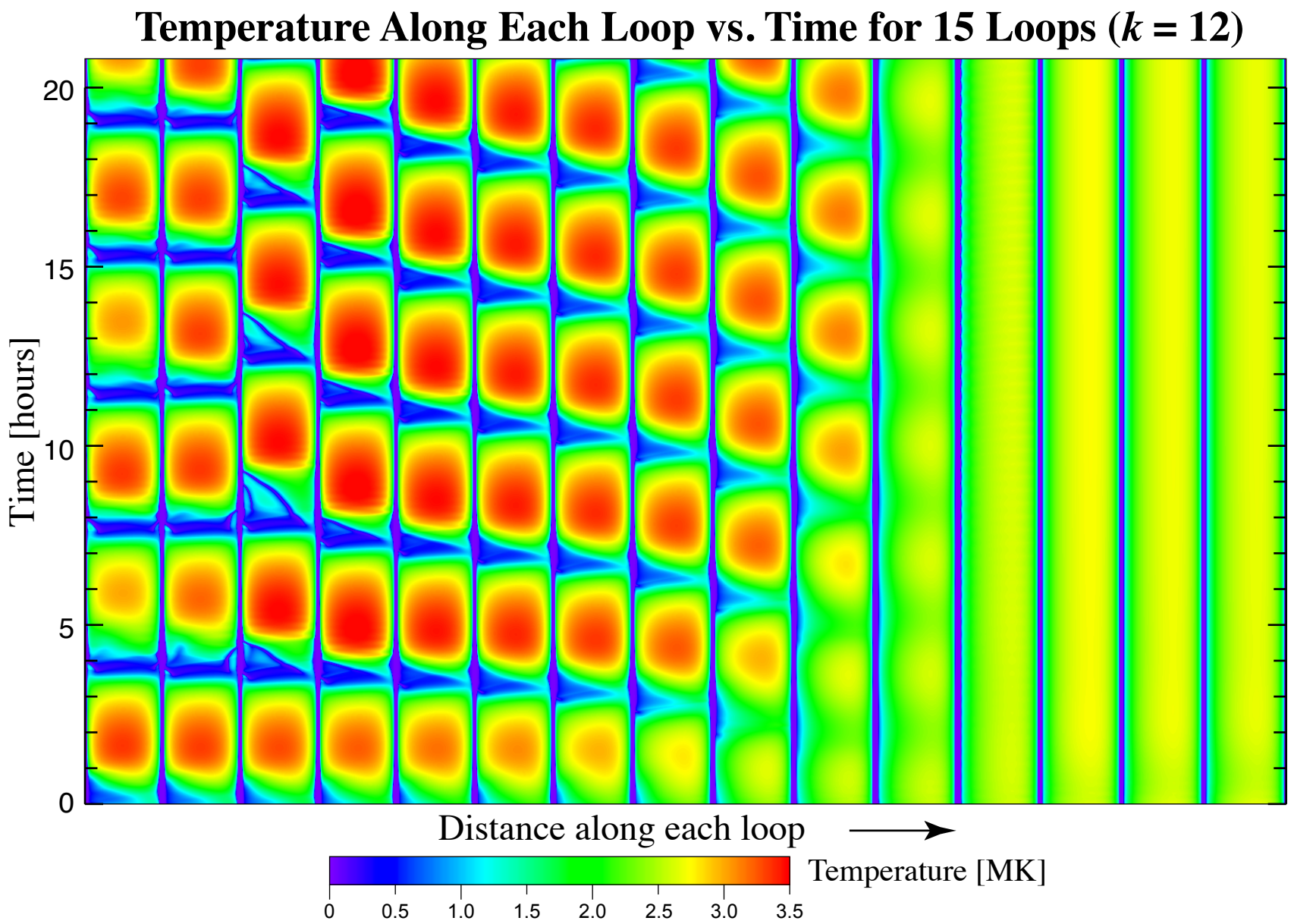
Temperature Along Each Loop vs. Time for 15 Loops (k = 12)
Time [hours]
0
5
10
15
20
Distance along each loop
Temperature [MK]
0
0.5
1.0
1.5
2.0
2.5
3.0
3.5

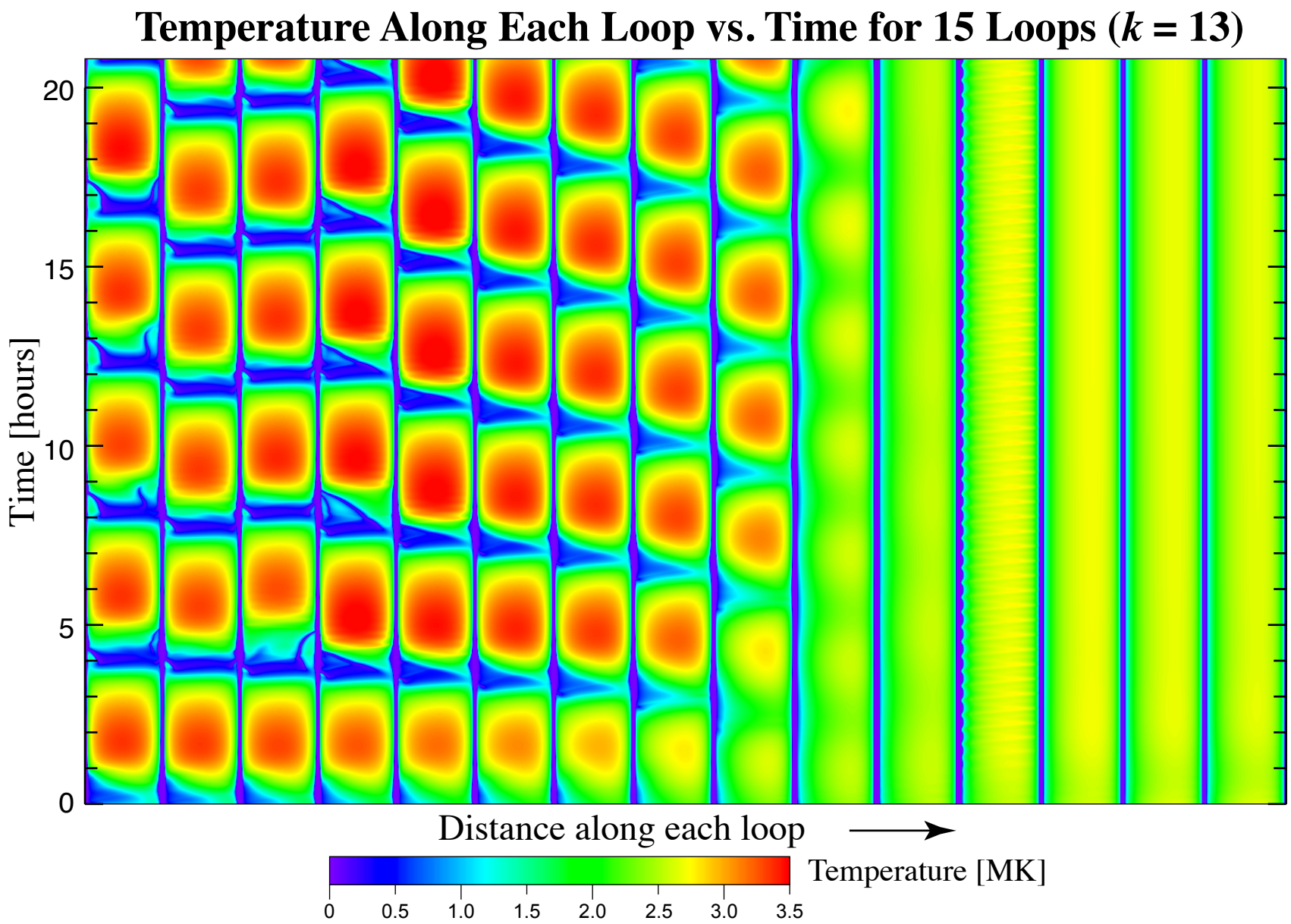
Temperature Along Each Loop vs. Time for 15 Loops (k = 13)
Time [hours]
0
5
10
15
20
Distance along each loop
Temperature [MK]
0
0.5
1.0
1.5
2.0
2.5
3.0
3.5

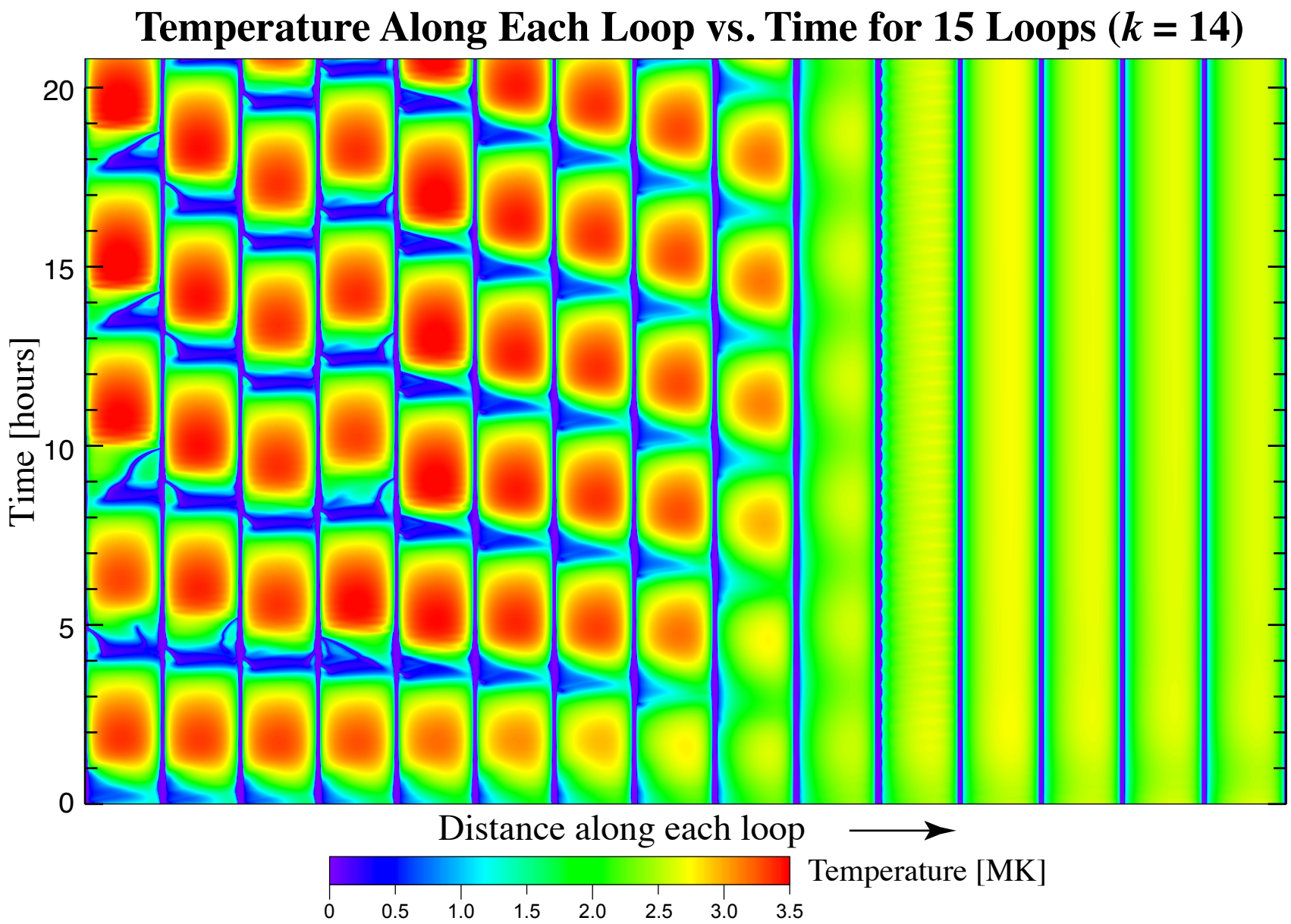
Temperature Along Each Loop vs. Time for 15 Loops (k = 14)
Time [hours]
0
5
10
15
20
Distance along each loop
Temperature [MK]
0
0.5
1.0
1.5
2.0
2.5
3.0
3.5

Temperature Along Each Loop vs. Time for 15 Loops (k = 15)

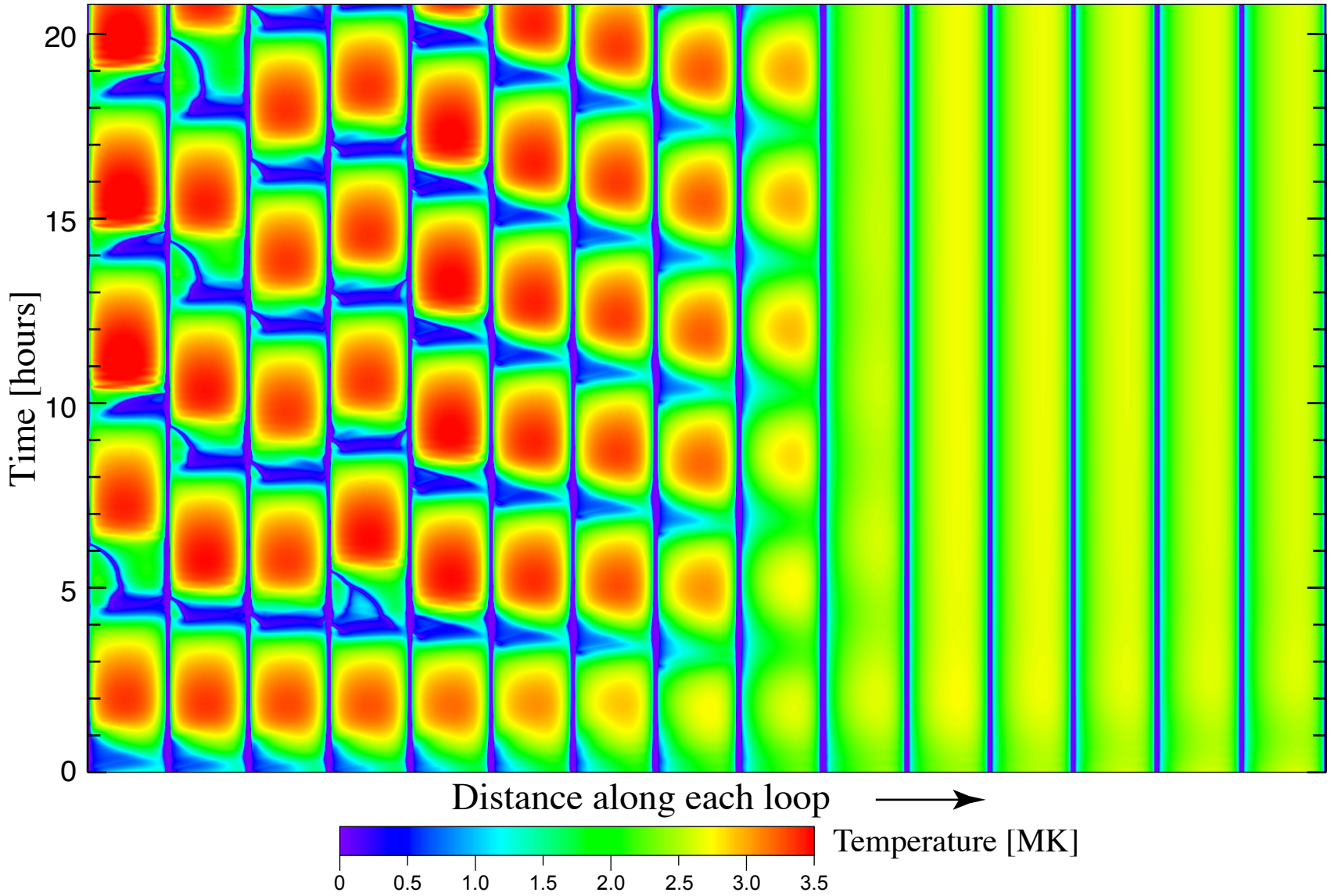

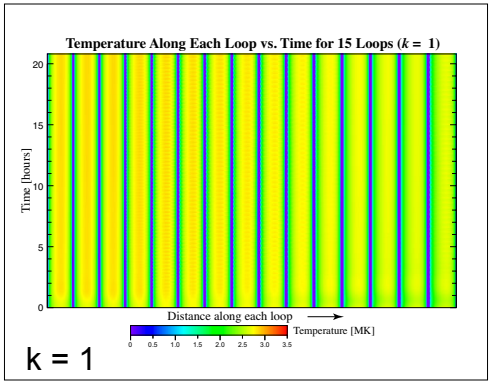

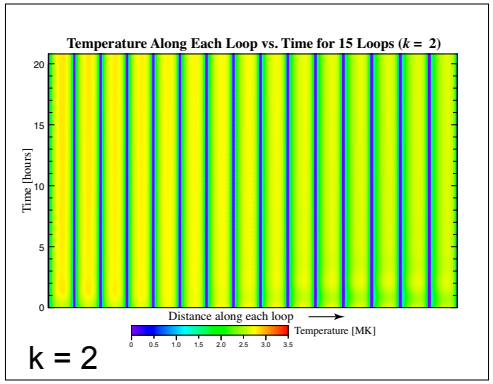

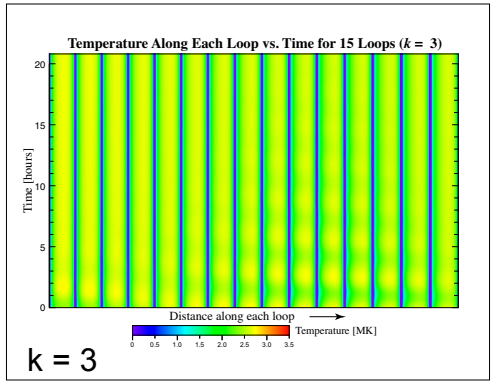

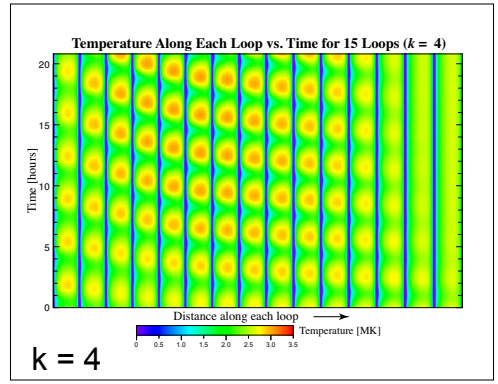

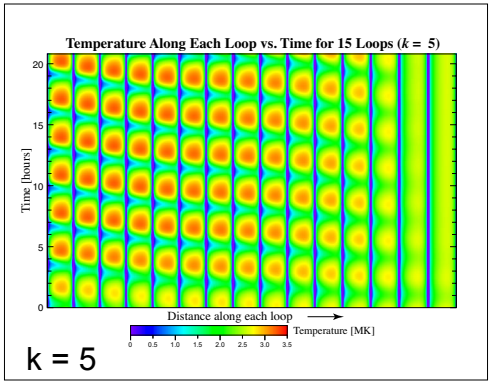

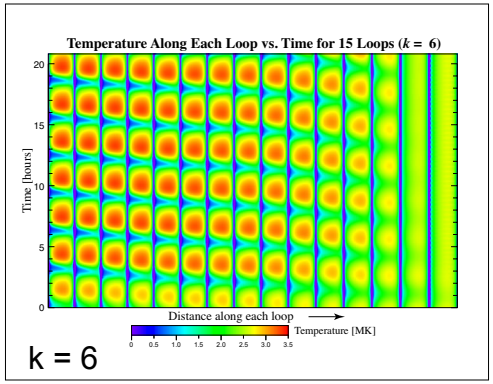

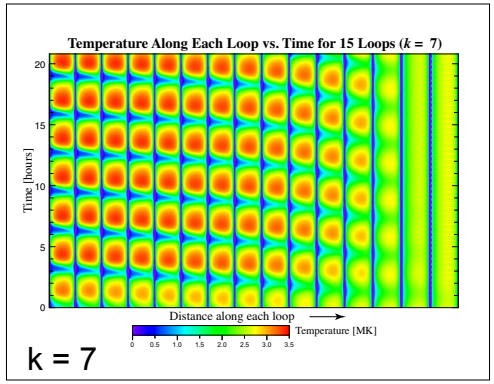

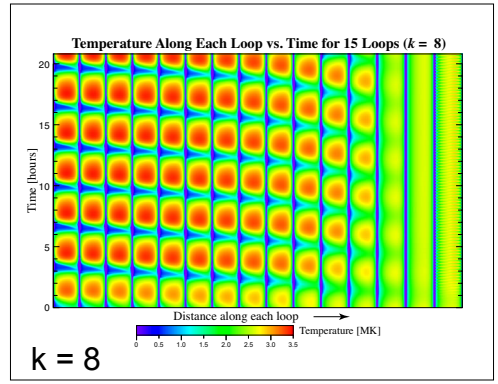

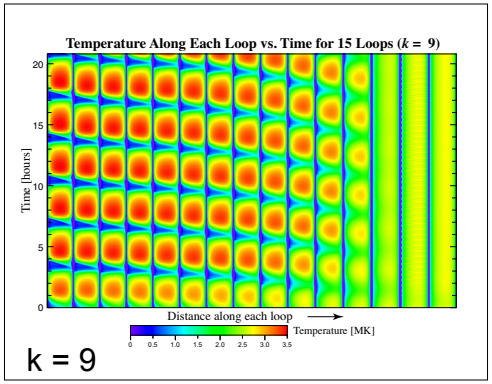

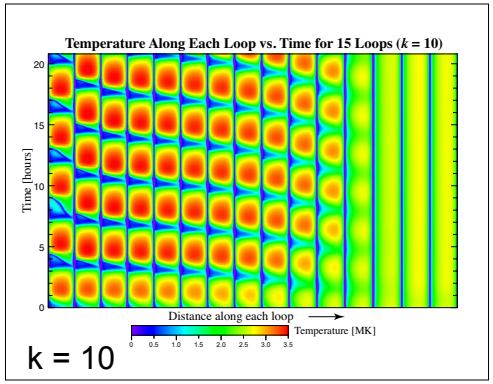

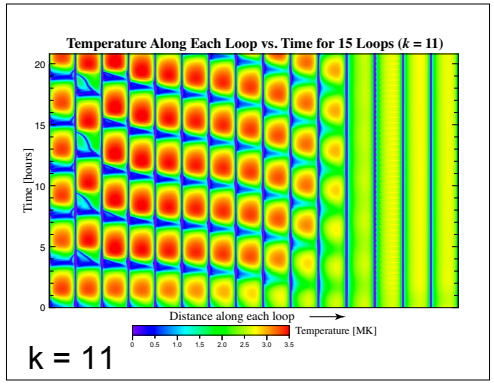

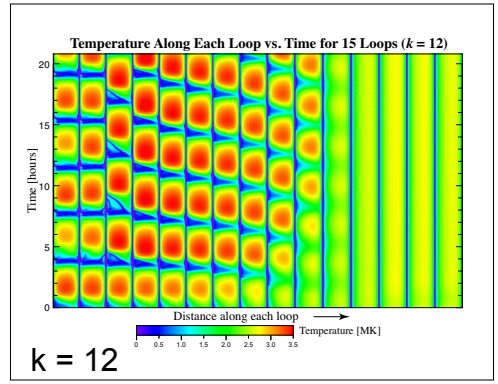

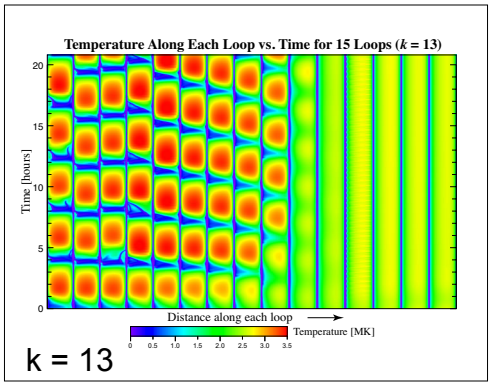

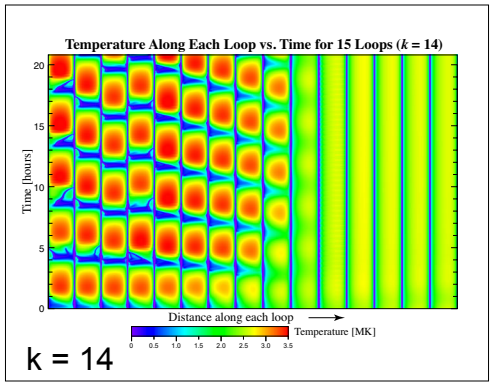

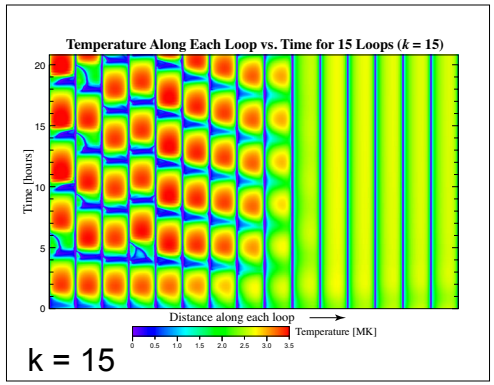

Of 225 loops, 140 experienced thermal nonequilibrium (62%), and 85 were stable.

TRANSITION BETWEEN COMPLETE AND INCOMPLETE CONDENSATIONS

- Consider a heating profile that is concentrated at the loop footpoints:

$$H(s) = H_0 + H_1(e^{-g(s)/\lambda} + e^{-g(L-s)/\lambda}),$$

with $H_1 = 45 \times 10^{-4}$ erg/cm^3/s, and $\lambda = 10$ Mm.
[$g(s) = \max(s - \Delta, 0)$, with $\Delta = 5$ Mm, is introduced to flat-top the heating in the chromosphere.]

- Consider two models that have different H_o values:
  - Model 1 has $H_o = 6 \times 10^{-4}$ erg/cm^3/s;
  - Model 2 has $H_o = 2 \times 10^{-4}$ erg/cm^3/s.
- The solution for Model 1 has an incomplete condensation, whereas the solution for Model 2 has a complete condensation [like those discussed by Klimchuk *et al*. (2010)]. These solutions are described by Mikić *et al*. (2013).
- The transition can be studied by varying H_o.

Symmetric Loop Profiles

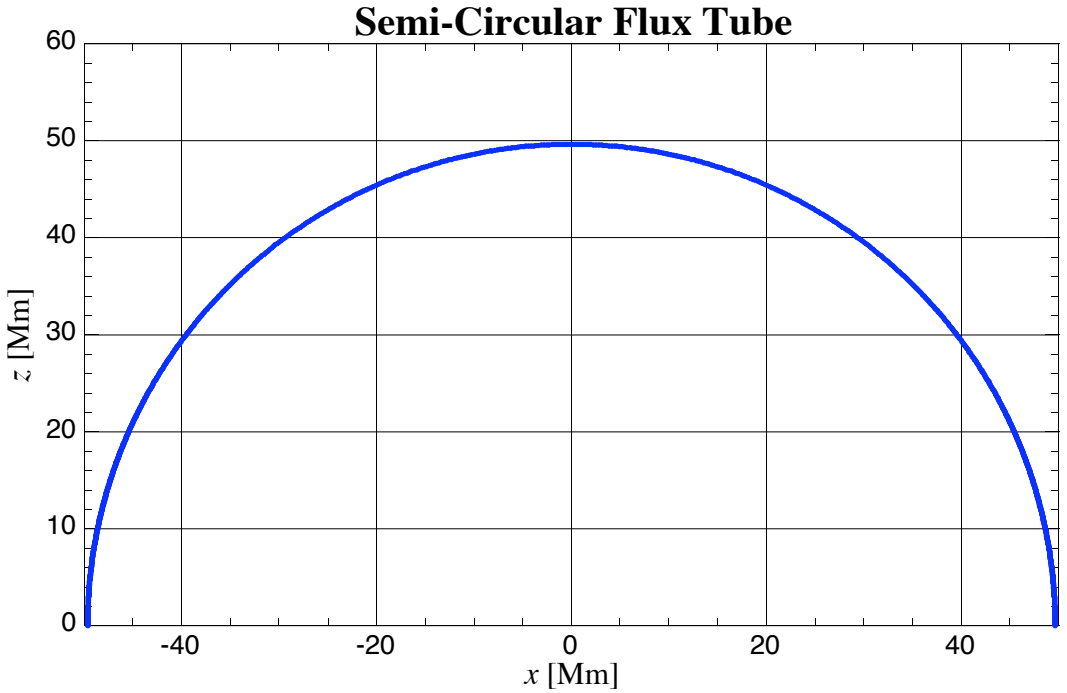

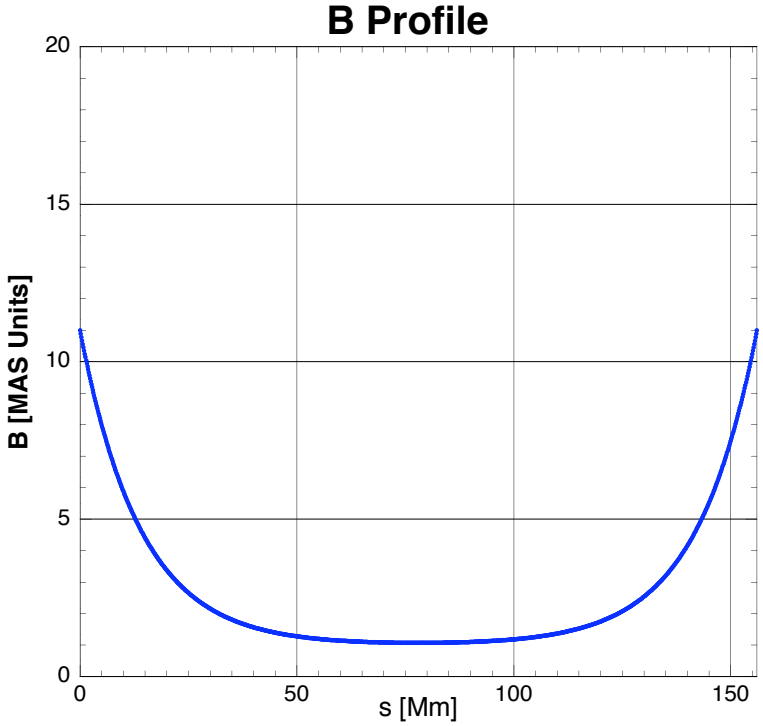

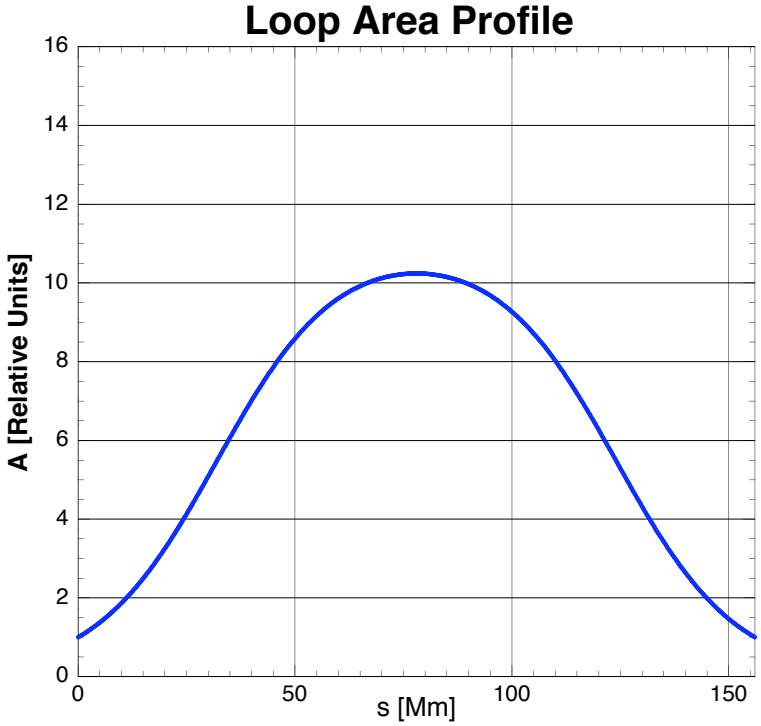

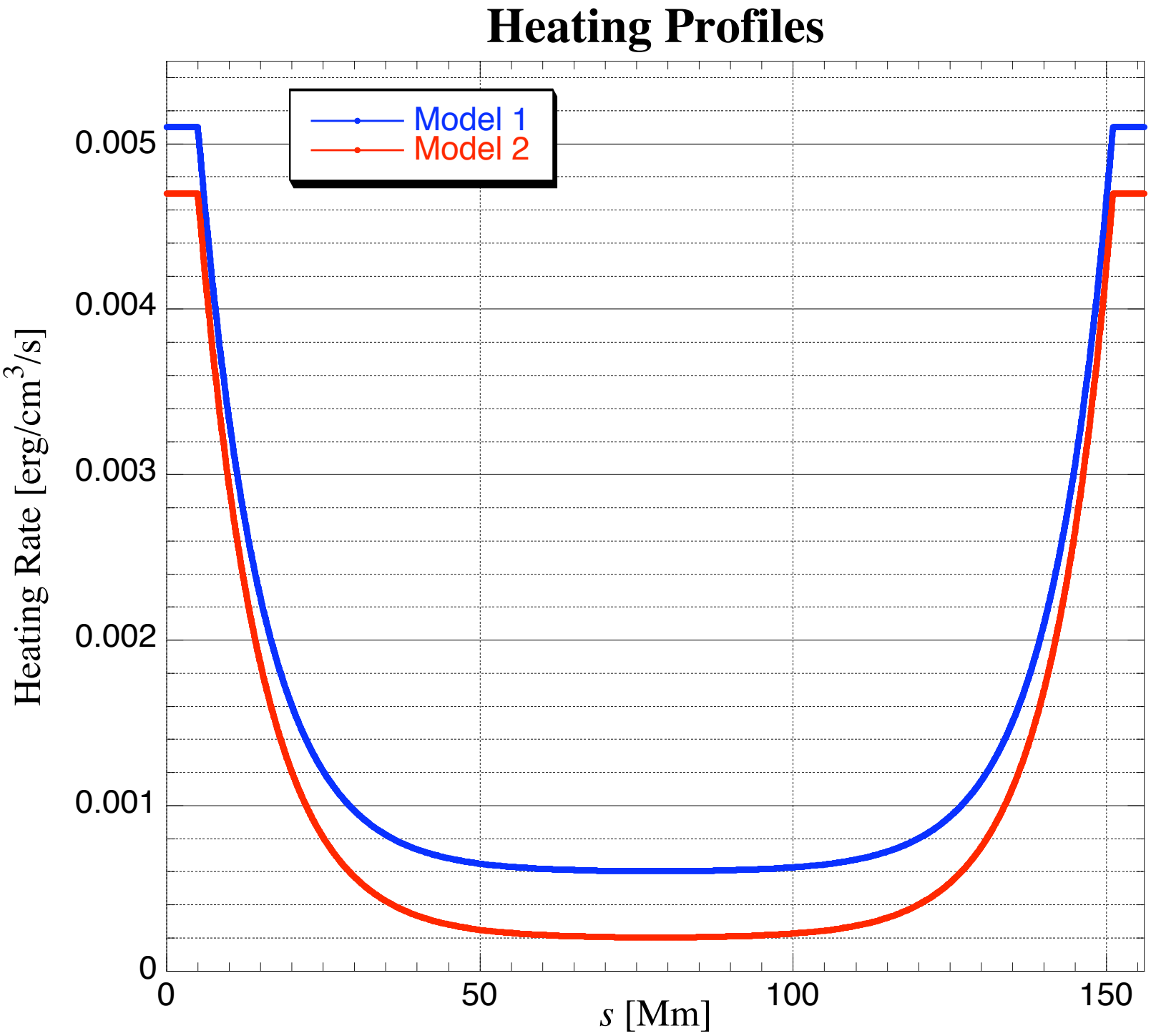
Heating Profiles
Model 1
Model 2
0.005
0.004
0.003
0.002
0.001
0
Heating Rate [erg/cm3/s]
0
50
100
150
s [Mm]

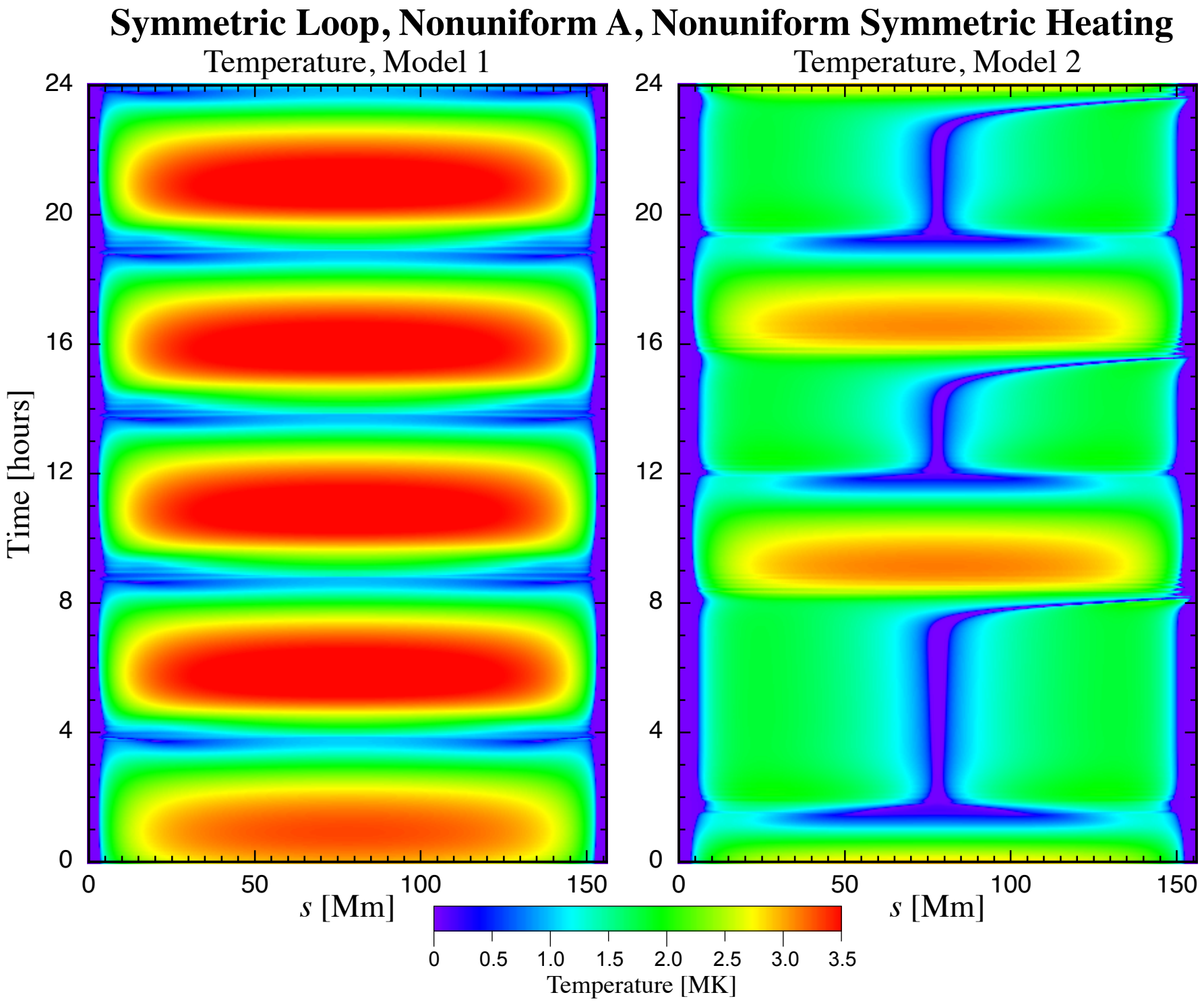
Symmetric Loop, Nonuniform A, Nonuniform Symmetric Heating
Temperature, Model 1
Temperature, Model 2
Time [hours]
24
20
16
12
8
4
0
0
50
100
150
s [Mm]
s [Mm]
0
0.5
1.0
1.5
2.0
2.5
3.0
3.5
Temperature [MK]

INCOMPLETE CONDENSATION

(Model 1: $H_o = 6 \times 10^{-4}$ erg/cm^3/s)

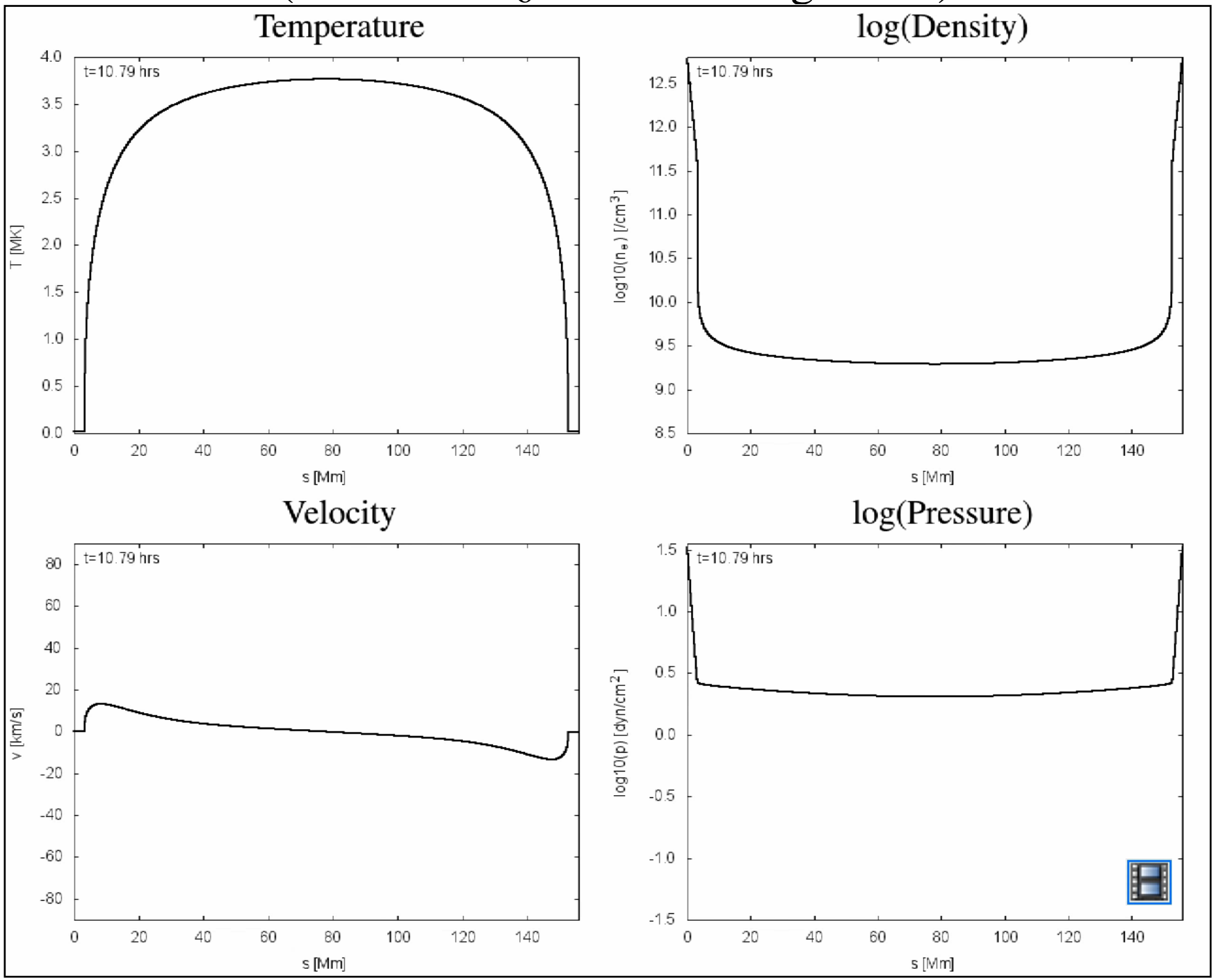

COMPLETE CONDENSATION

(Model 2: $H_o = 2 \times 10^{-4}$ erg/cm^3/s)

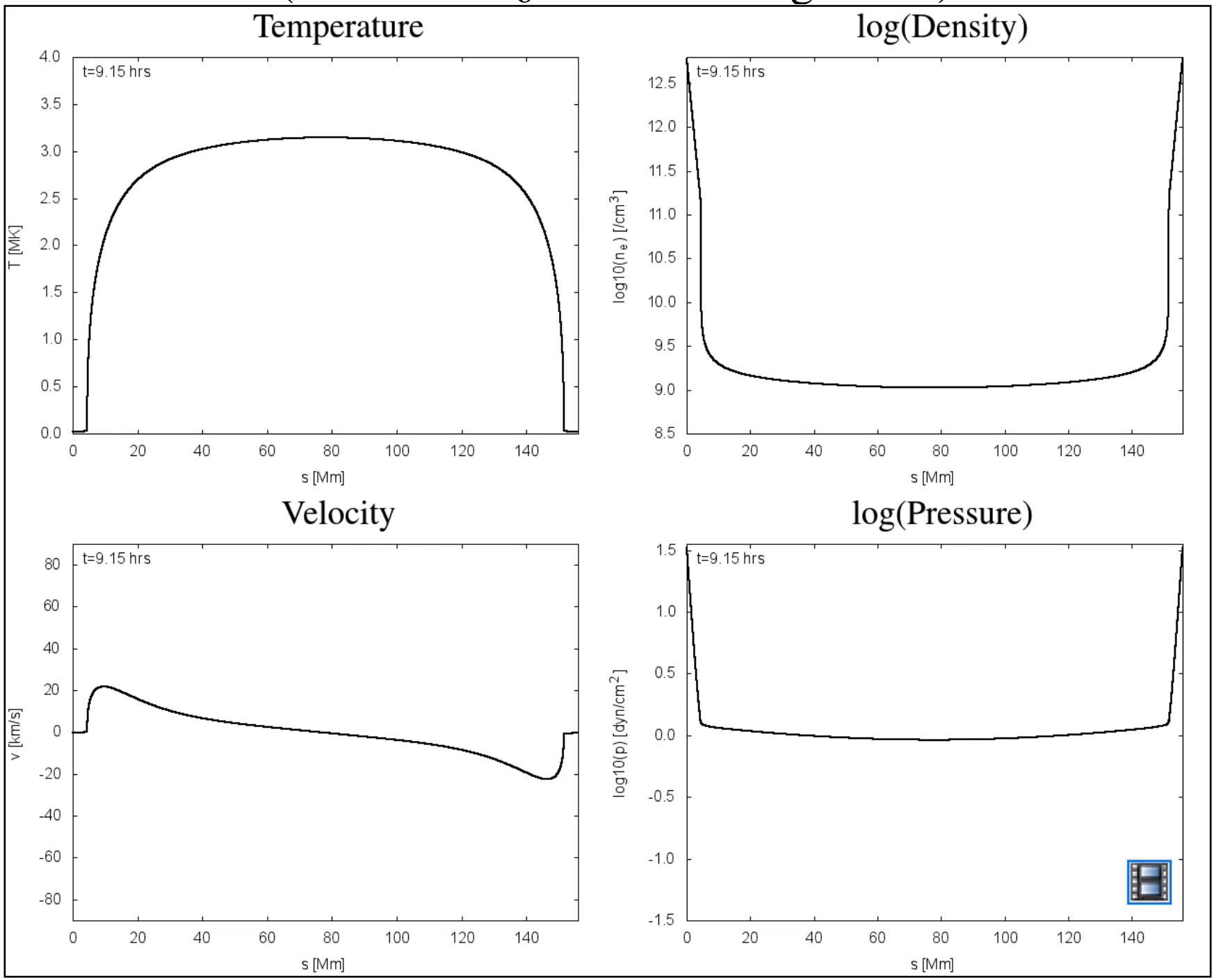

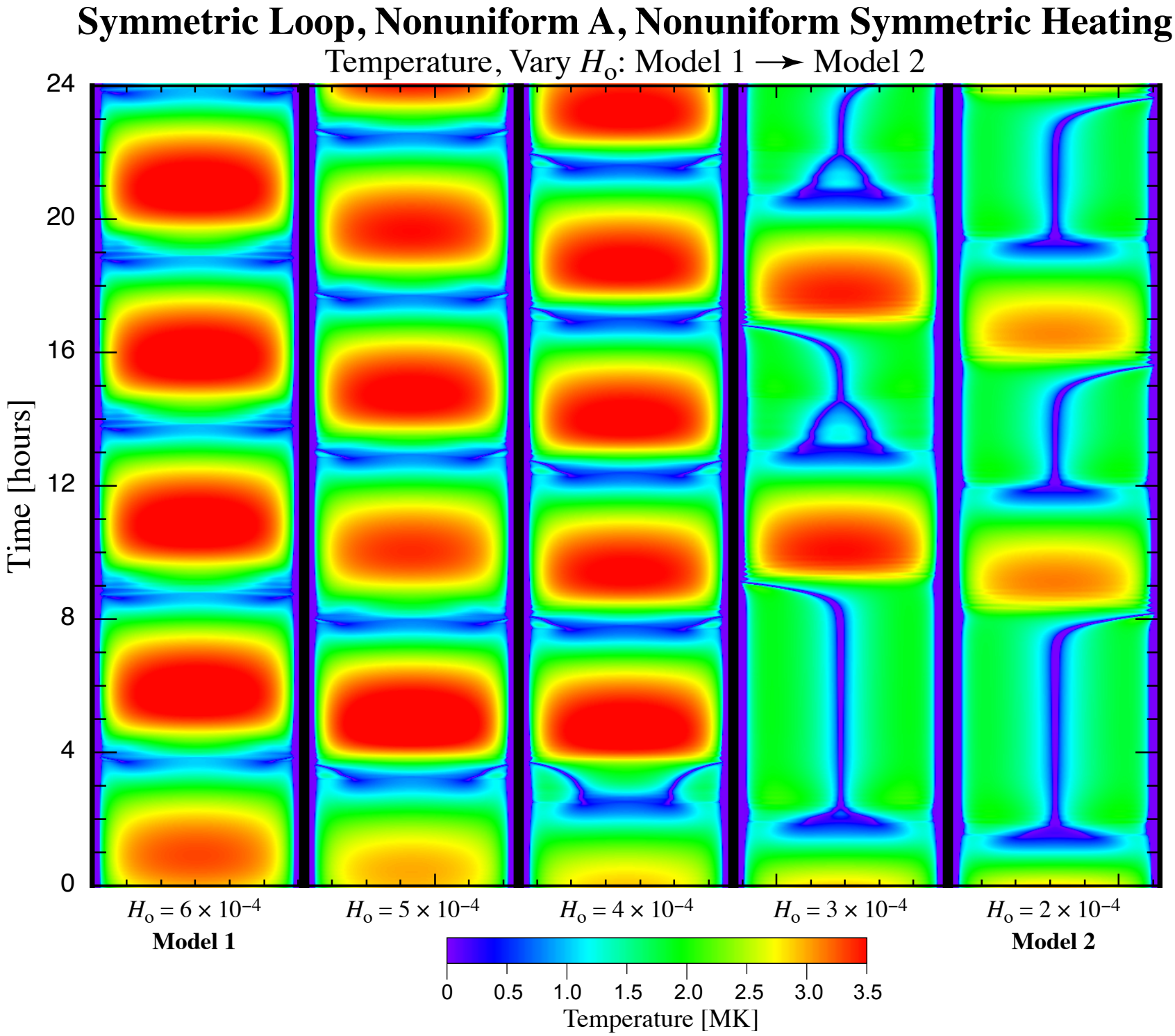
Symmetric Loop, Nonuniform A, Nonuniform Symmetric Heating
Temperature, Vary H_o: Model 1 → Model 2
Time [hours]
24
20
16
12
8
4
0
$H_o = 6 \times 10^{-4}$
$H_o = 5 \times 10^{-4}$
$H_o = 4 \times 10^{-4}$
$H_o = 3 \times 10^{-4}$
$H_o = 2 \times 10^{-4}$
Model 1
Model 2
0
0.5
1.0
1.5
2.0
2.5
3.0
3.5
Temperature [MK]

Now make the loop nonsymmetric (in shape, area, and heating) ...

Symmetric ⟶ Nonsymmetric Loop Profiles

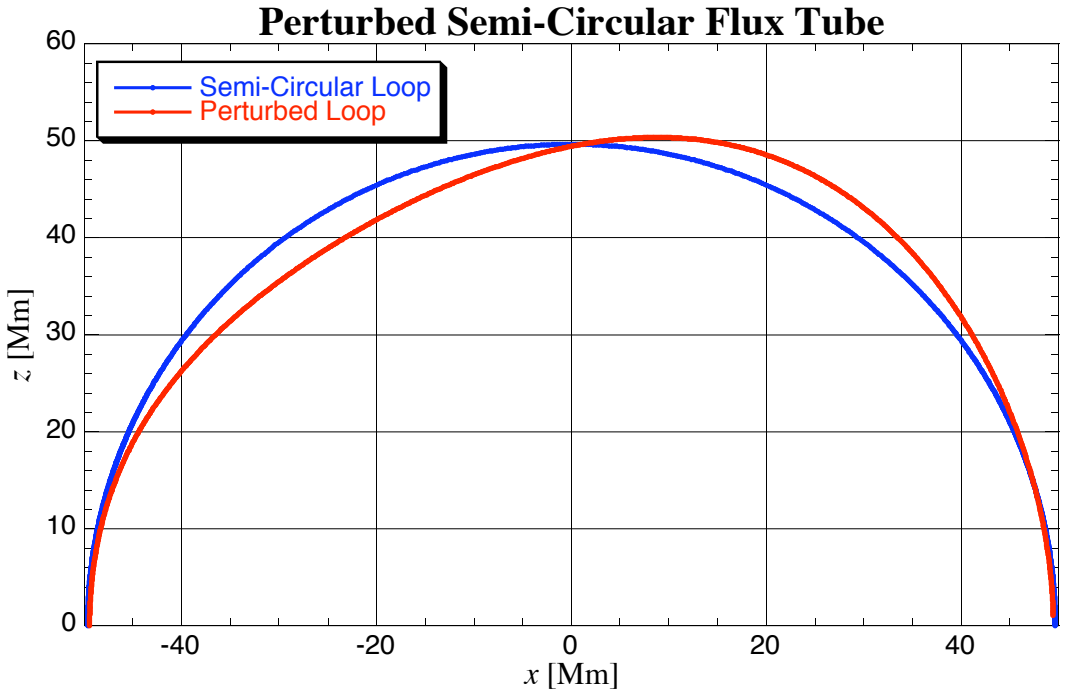

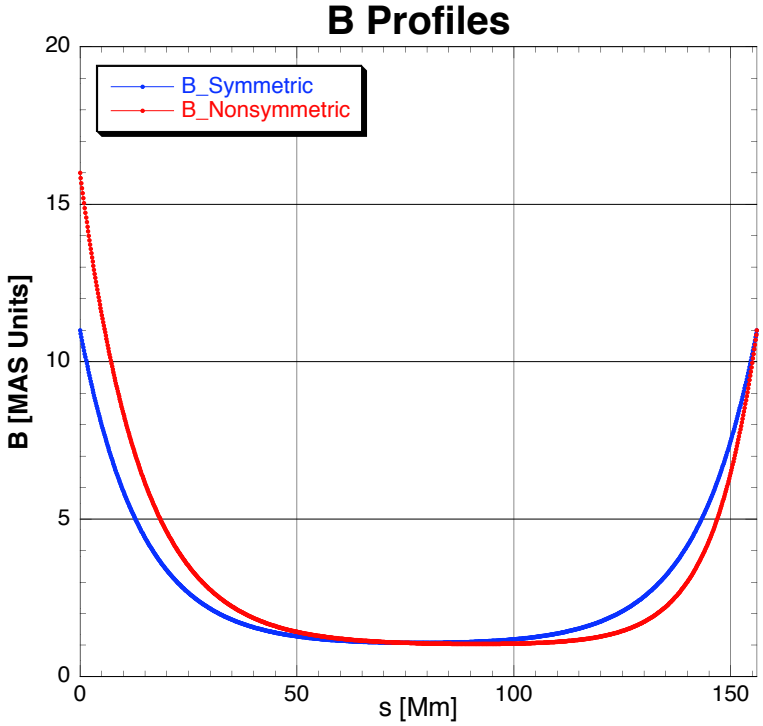

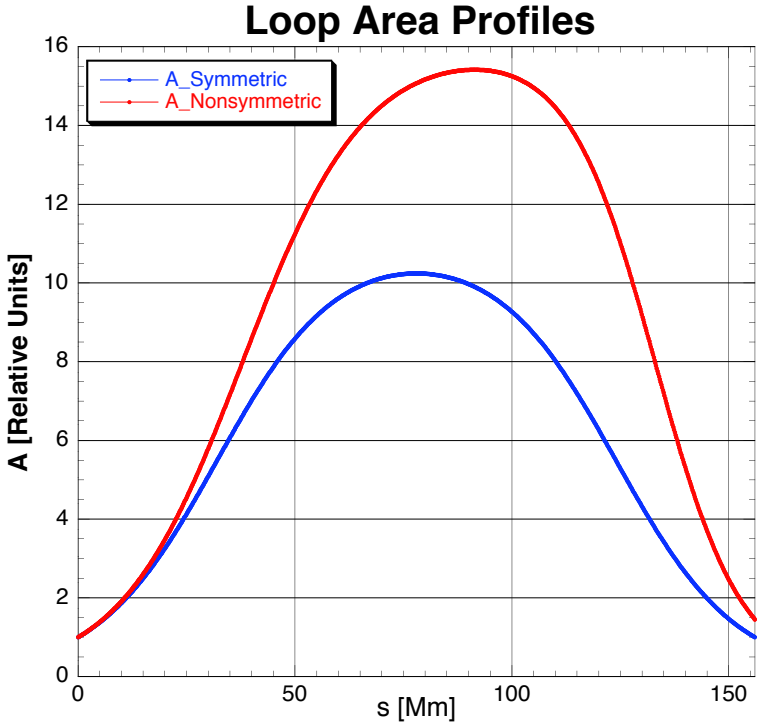

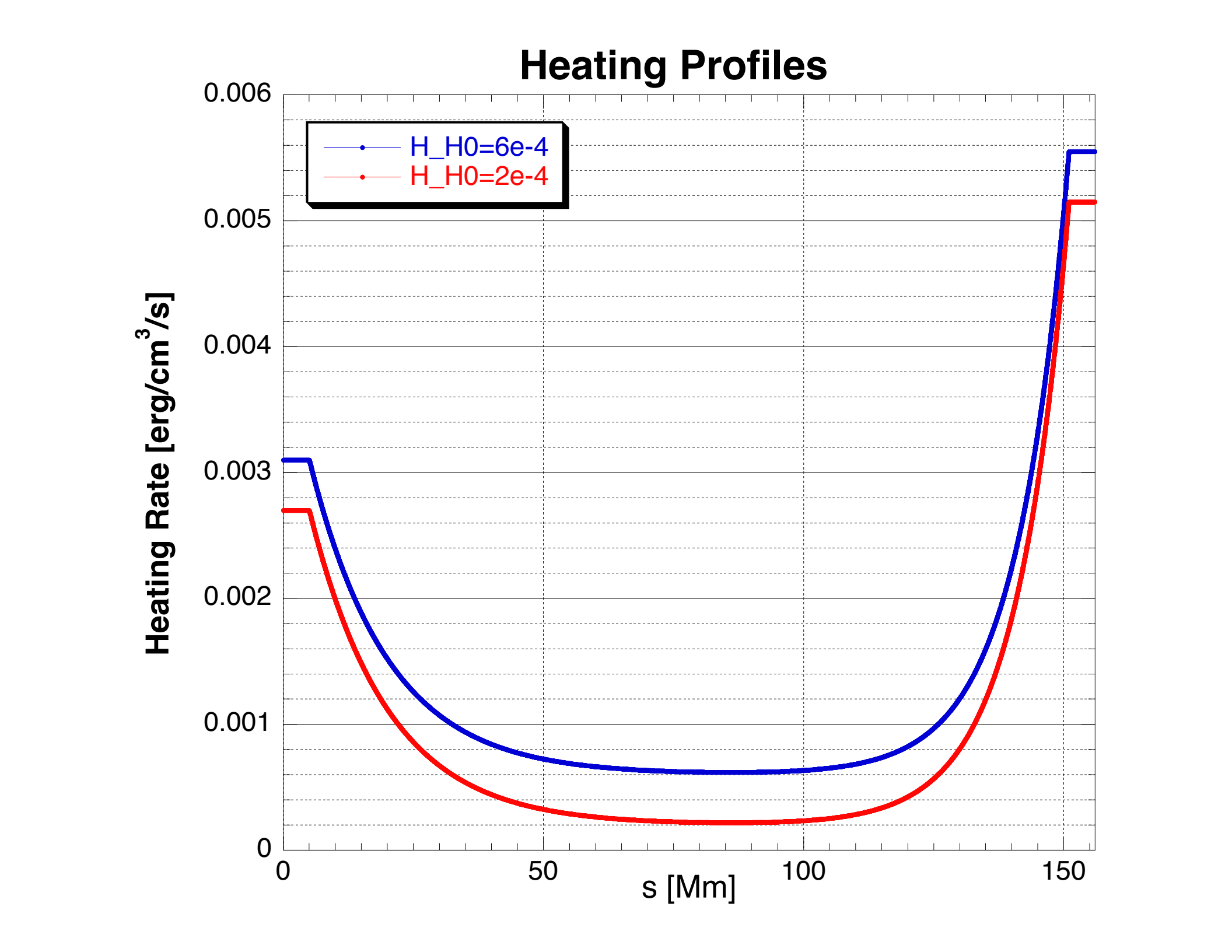
Heating Profiles
H_H0=6e-4
H_H0=2e-4
Heating Rate [erg/cm3/s]
0.006
0.005
0.004
0.003
0.002
0.001
0
0
50
100
150
s [Mm]

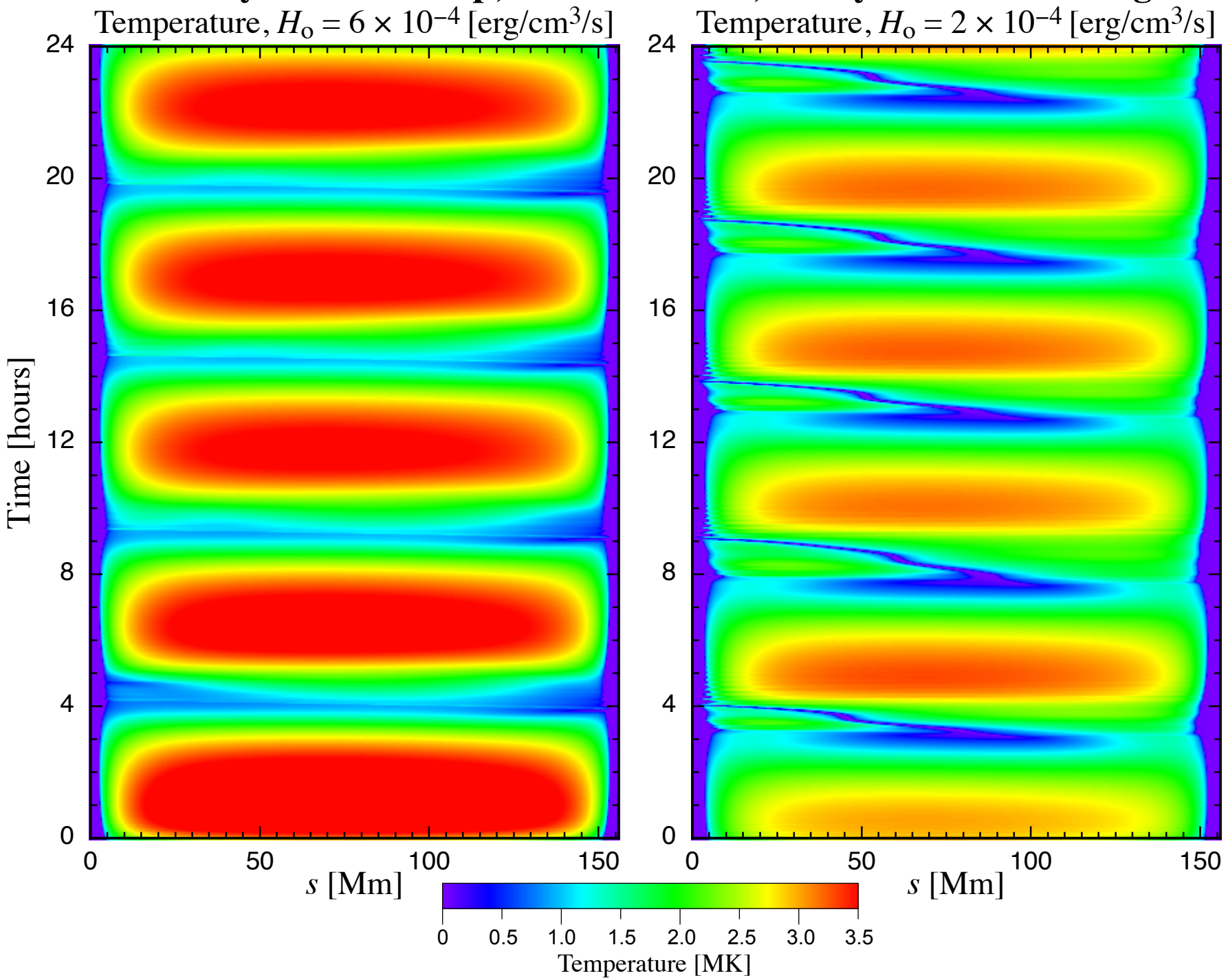
Nonsymmetric Loop, Nonuniform A, Nonsymmetric Heating
Temperature, $H_o = 6 \times 10^{-4}$ [erg/cm^3/s]
Temperature, $H_o = 2 \times 10^{-4}$ [erg/cm^3/s]
Time [hours]
0
4
8
12
16
20
24
0
50
100
150
s [Mm]
0
0.5
1.0
1.5
2.0
2.5
3.0
3.5
Temperature [MK]

INCOMPLETE CONDENSATION

(Nonsymmetric Shape, A, and H: $H_o = 6 \times 10^{-4}$ erg/cm^3/s)

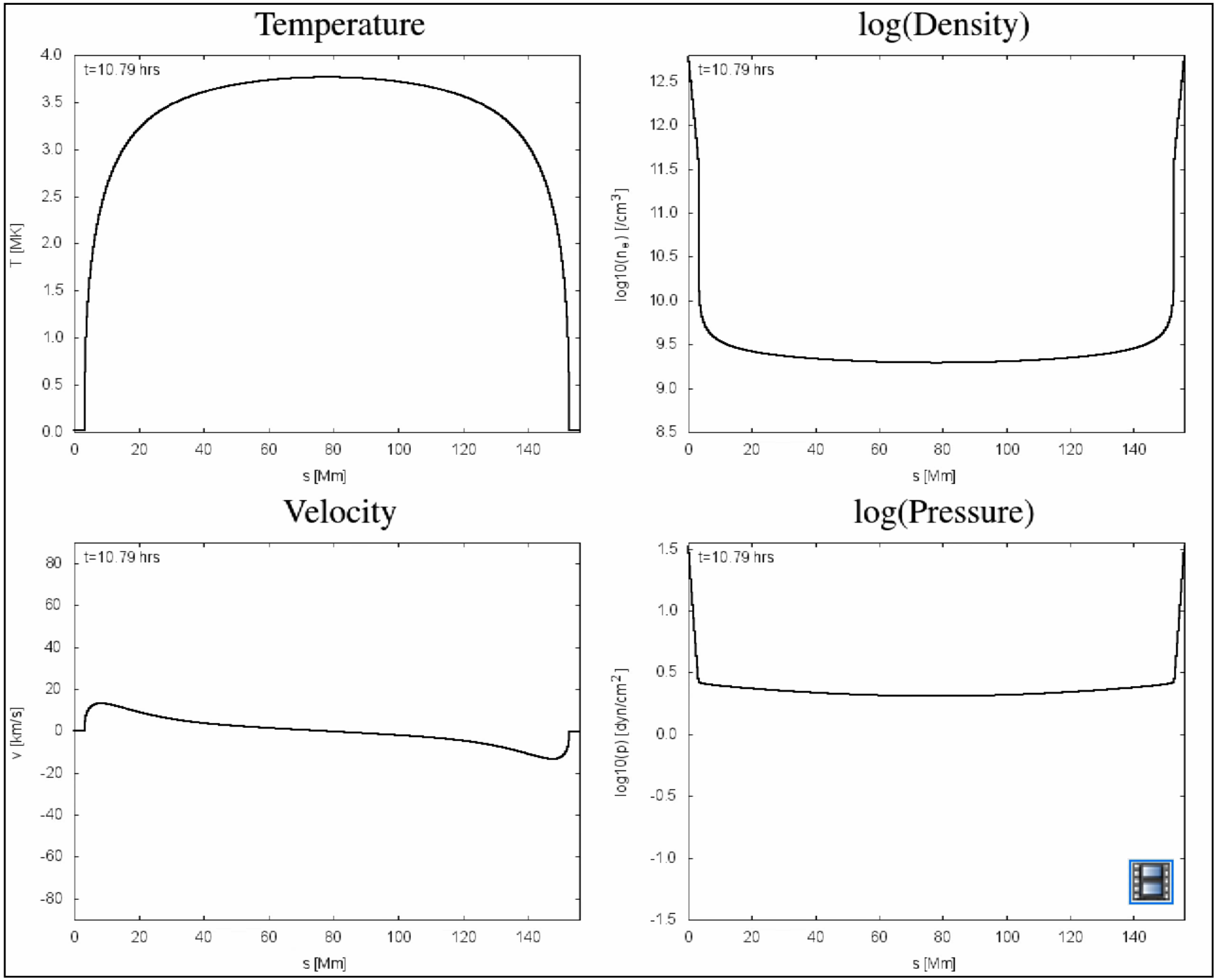

COMPLETE CONDENSATION

(Nonsymmetric Shape, A, and H: $H_o = 2 \times 10^{-4}$ erg/cm^3/s)

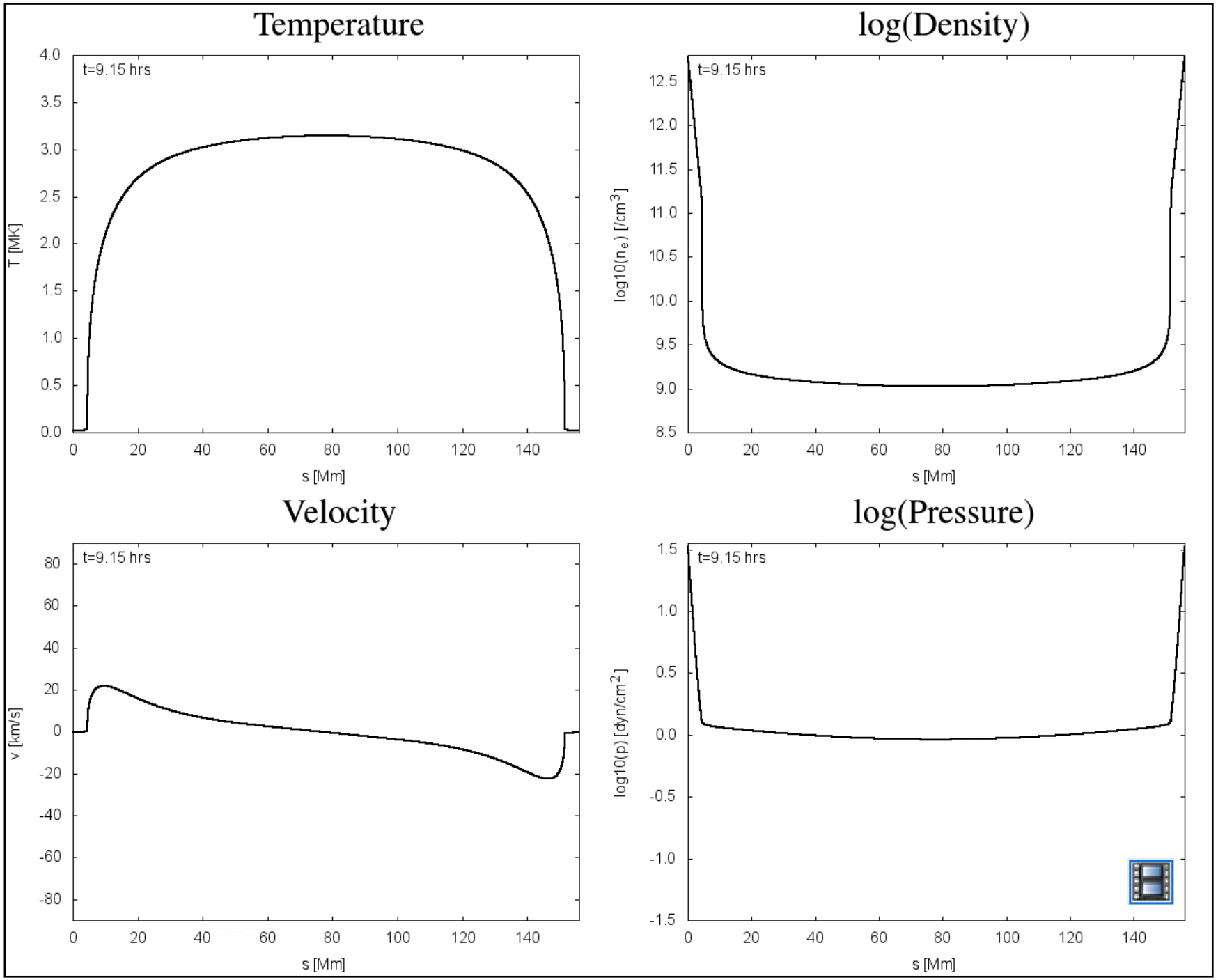

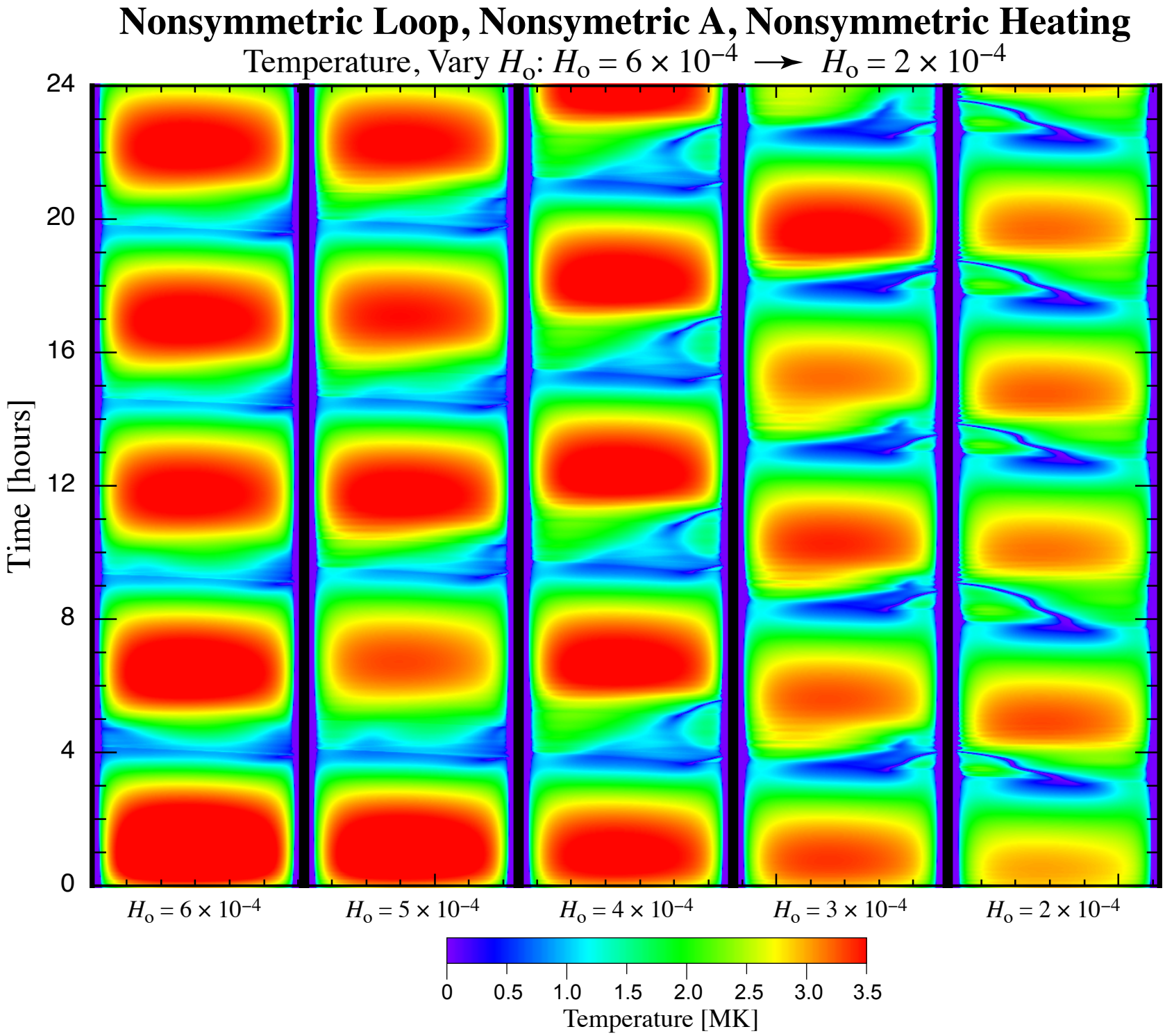
Nonsymmetric Loop, Nonsymetric A, Nonsymmetric Heating
Temperature, Vary H_o: $H_o = 6 \times 10^{-4}$ → $H_o = 2 \times 10^{-4}$
Time [hours]
24
20
16
12
8
4
0
$H_o = 6 \times 10^{-4}$
$H_o = 5 \times 10^{-4}$
$H_o = 4 \times 10^{-4}$
$H_o = 3 \times 10^{-4}$
$H_o = 2 \times 10^{-4}$
0
0.5
1.0
1.5
2.0
2.5
3.0
3.5
Temperature [MK]

DETAILED INVESTIGATION:
AR 11339: 08-NOV-2011, 19:12UT

- Bipolar active region; AR loops in core, plus fan loops; near disk center (~ 20°N)
- Studied by Warren *et al*. (2012) and Ugarte-Urra & Warren (2014)
- Thomas Wiegelmann calculated an NLFFF solution
- The field in this solution appears to be very potential-looking
- Since the NLFFF had a rather tight "numerical box" surrounding it, we chose a potential field (over the whole Sun) for our study, since we would like to study the fan loops too
- There are good observations of this region: SDO AIA & HMI, Hinode XRT & EIS

AIA 171Å + 193Å + 211Å

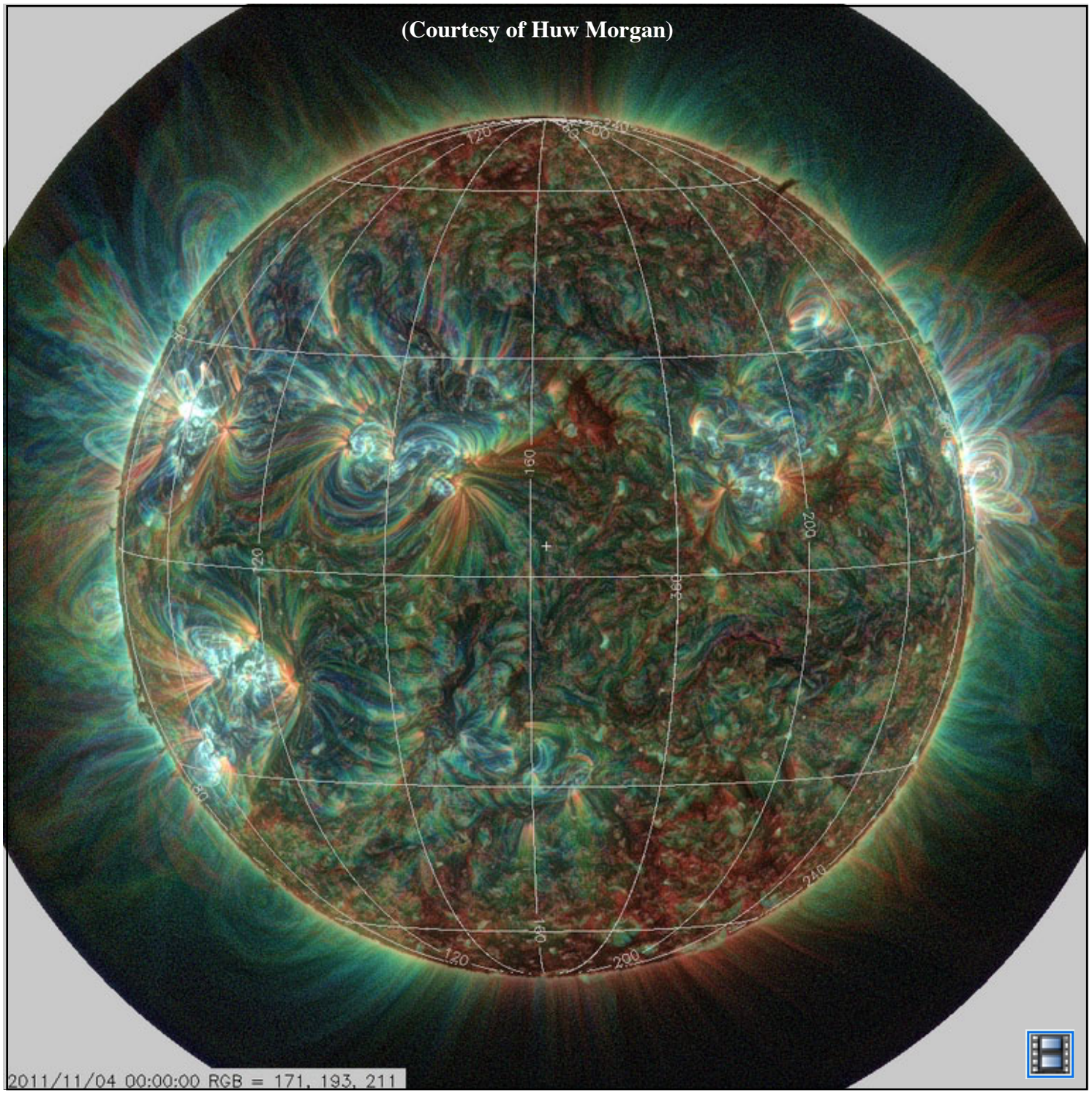

AIA 171Å + 193Å + 211Å
AR 11339: 2011/11/08 19:00UT

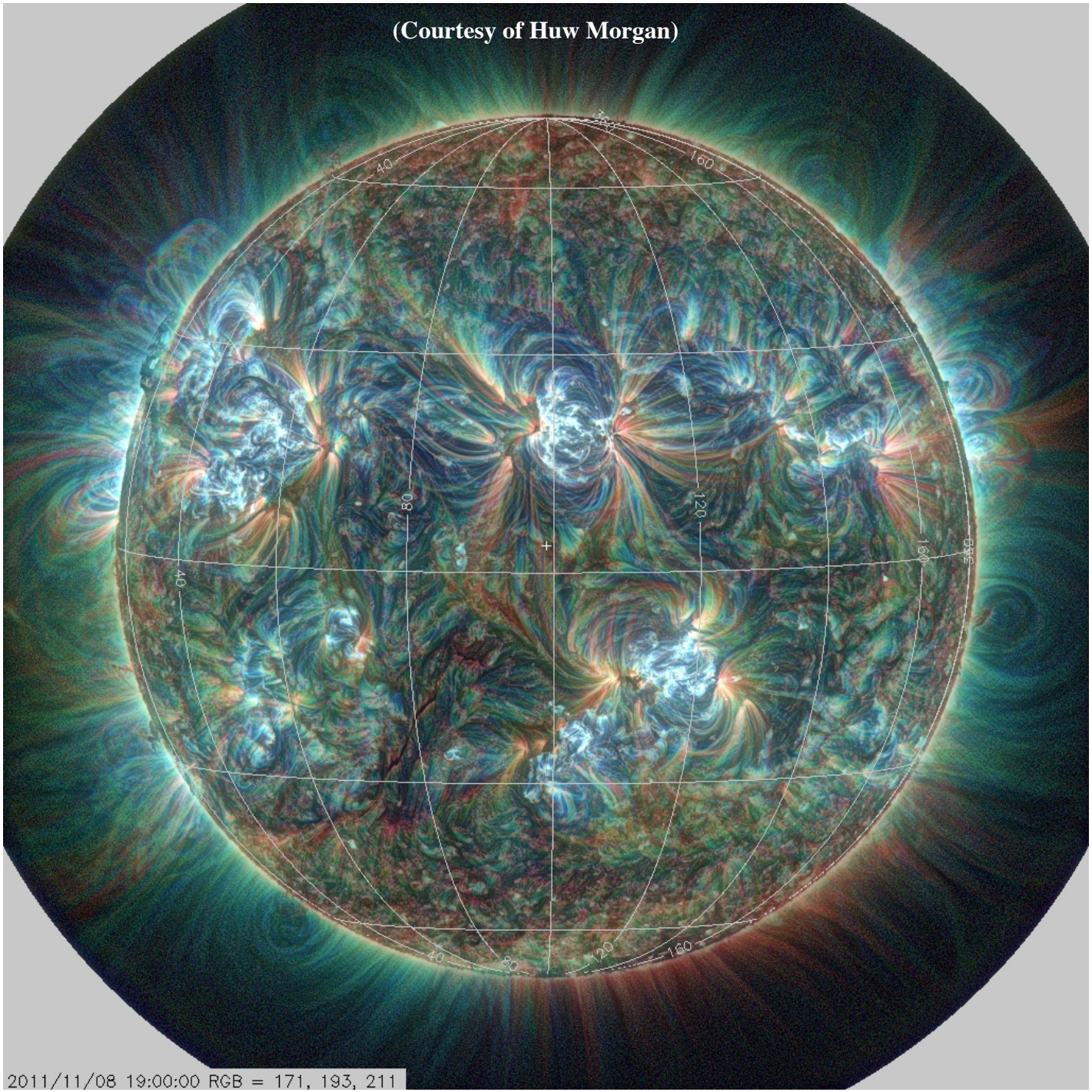

AIA 171Å + 193Å + 211Å
AR 11339: 2011/11/08 19:00UT

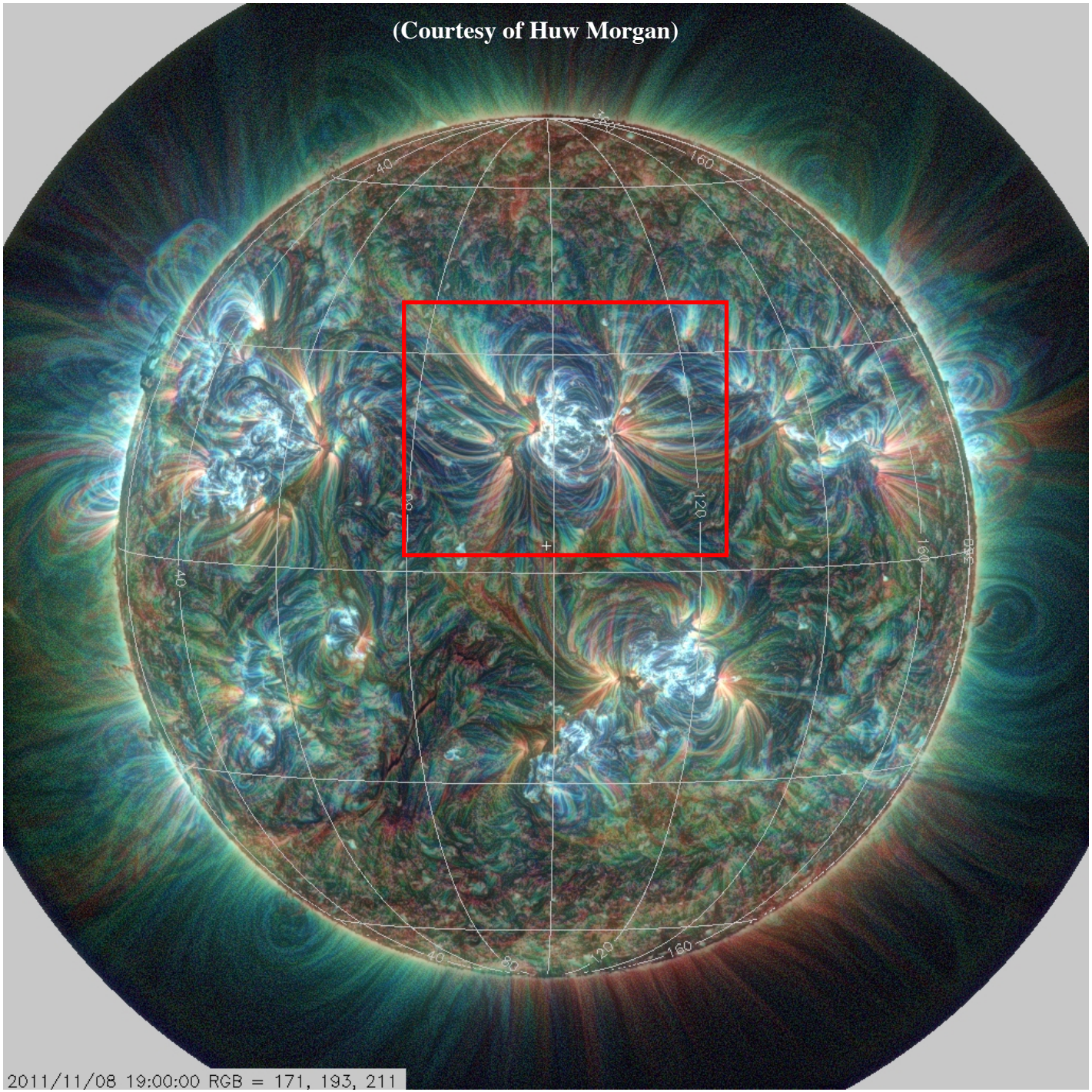

Blend of AIA Emission (171Å + 193Å + 211Å) and NLFFF Field Lines (Wiegelmann)

Blend of AIA Emission (171Å + 193Å + 211Å) and Potential Field Lines

Emission from AR11339

AIA 94Å

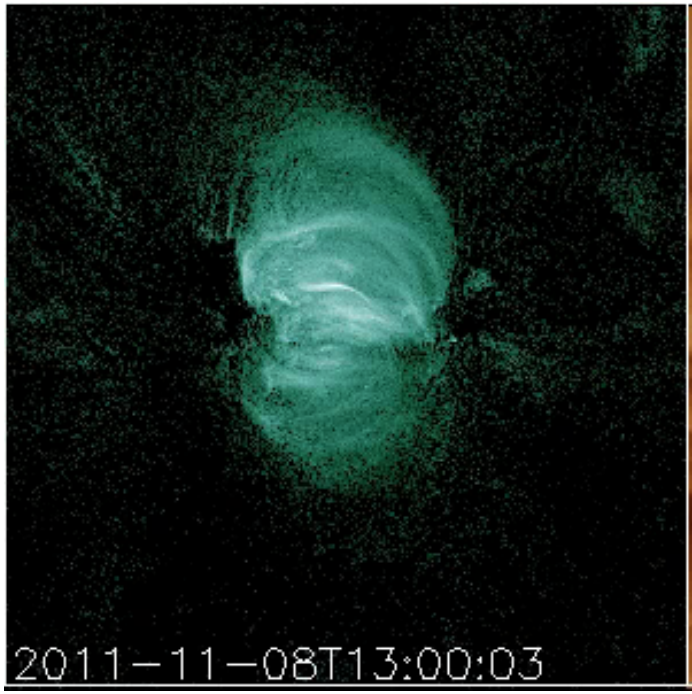

AIA 193Å

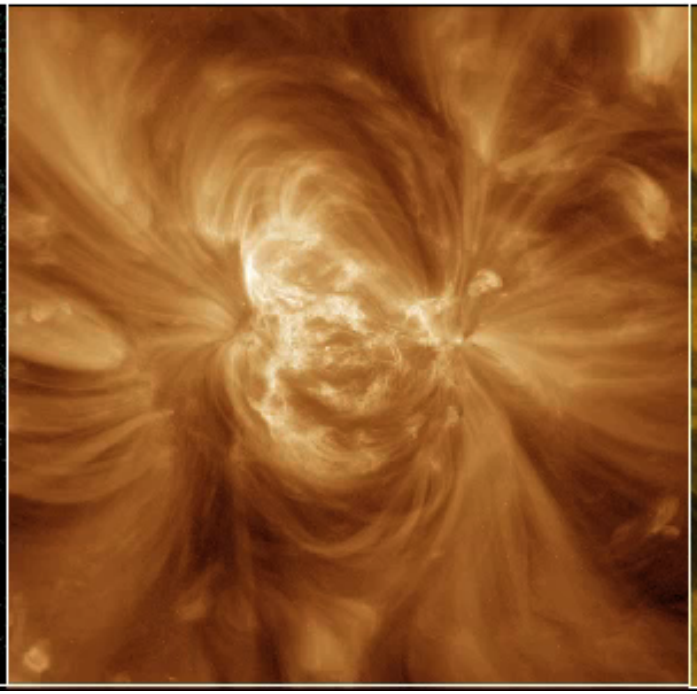

AIA 171Å

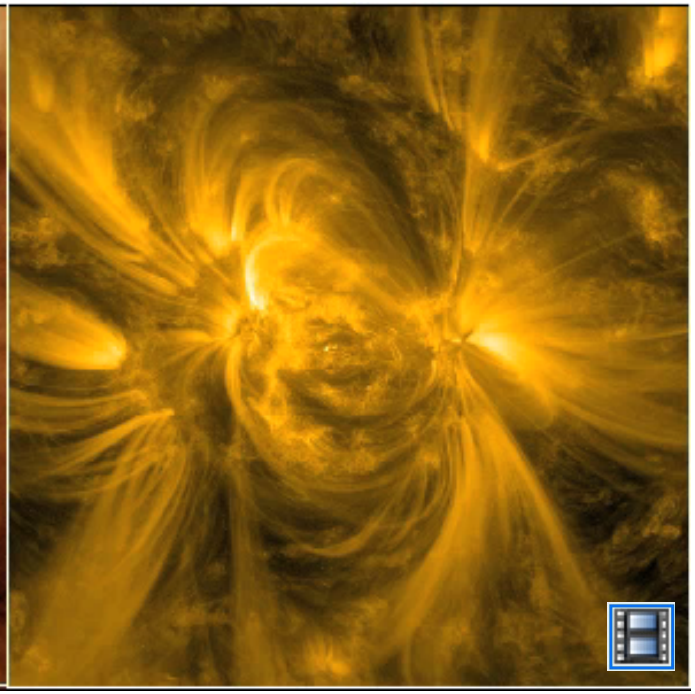

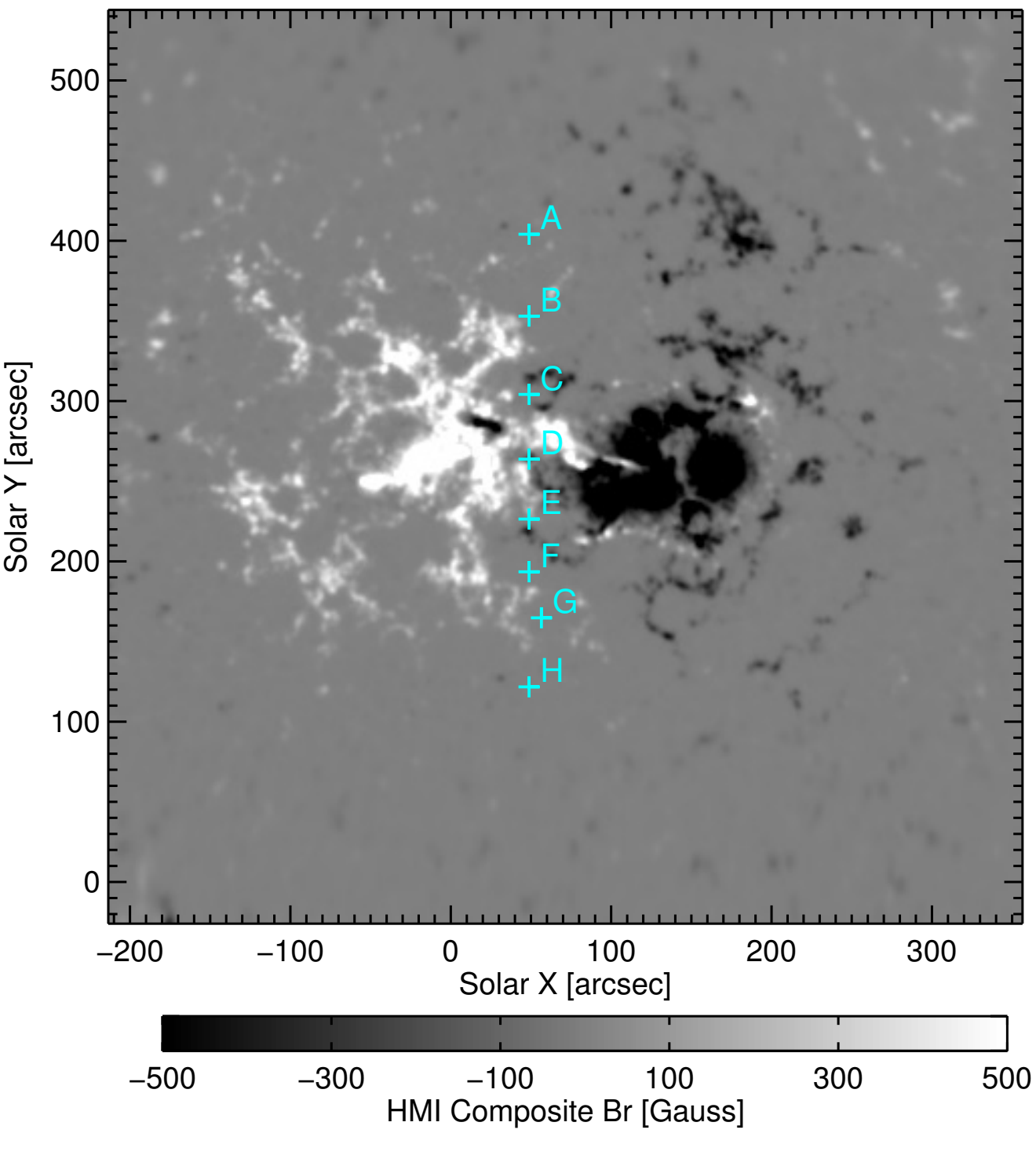
A
B
C
D
E
F
G
H
500
400
300
200
100
0
Solar Y [arcsec]
−200
−100
0
100
200
300
Solar X [arcsec]
−500
−300
−100
100
300
500
HMI Composite Br [Gauss]

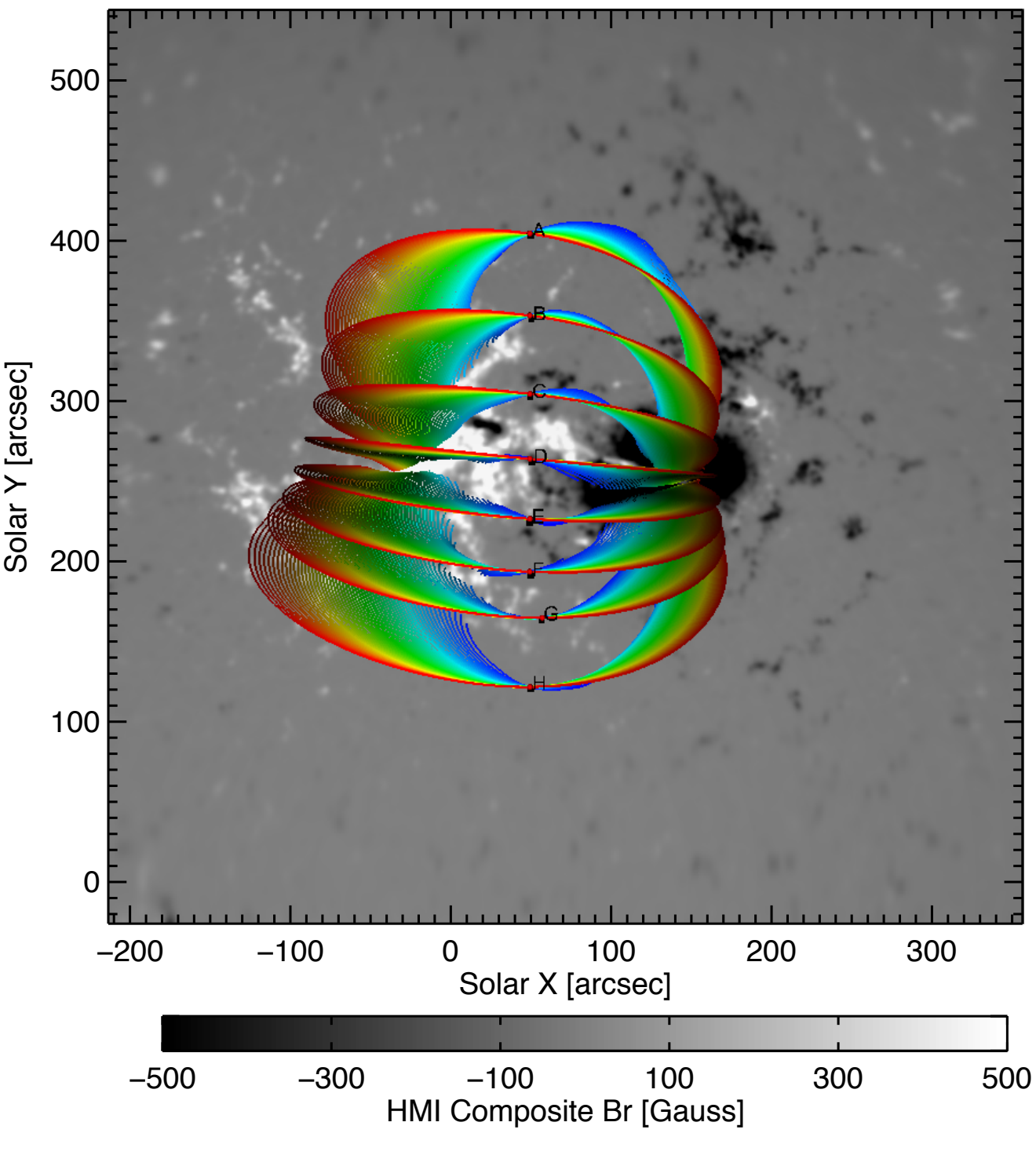
A
B
C
D
E
F
G
H
500
400
300
200
100
0
Solar Y [arcsec]
−200
−100
0
100
200
300
Solar X [arcsec]
−500
−300
−100
100
300
500
HMI Composite Br [Gauss]

METHODOLOGY

- We will contrast the behavior of 3 different coronal heating mechanisms:
  - An empirical heating model (Mok *et al*. 2016) inspired by the heating from weak MHD turbulence simulations (Rappazzo *et al*. 2007, 2008; Parker 1972), producing thermal nonequilibrium
  - Nanoflare heating (e.g., Parker 1988; Cargill & Klimchuk 1997, 2004; Klimchuk & Cargill 2001; Klimchuk 2006; Warren *et al*. 2003, 2011; Cargill 2014; Cargill *et al*. 2015)
  - Wave-Turbulence-Driven (WTD) heating (Matthaeus *et al*. 1999; Verdini & Velli 2007; Verdini *et al*. 2010; Lionello *et al*. 2014; Downs *et al*. 2016)

DIAGNOSTICS

- We will use the following diagnostics:
  - Time delays between different EUV and X-ray channels (e.g., Viall & Klimchuk 2012, 2013) [see the talk by Amy Winebarger at this meeting]
  - Ratios of peak intensities between channels
  - DEMs
- The idea is to understand the fundamental signatures of these different heating mechanisms so that we can unravel their possible presence in observations

CONCLUSIONS

- When active regions are heated to match observed EUV and X-ray emission, with certain types of coronal heating profiles, some of the loops undergo thermal nonequilibrium
- The solutions sometimes have complete (full) condensations high in the corona, but, perhaps more frequently, they can have incomplete condensations
- Such solutions may be able to explain observations
- The prevalence of thermal nonequilibrium in the corona has not been fully investigated
- There is a lot of work to be done to sort this out …